BUB1 mediation of caspase-independent mitotic death determines cell fate

Yohei Niikura,[1] Amruta Dixit,[2] Ray Scott,[2] Guy Perkins,[2] and Katsumi Kitagawa[1]

[1]Department of Molecular Pharmacology, St. Jude Children's Research Hospital, Memphis, TN 38105
[2]National Center for Microscopy and Imaging Research, Center for Research on Biological Structure, School of Medicine, University of California, San Diego, La Jolla, CA 92093

The spindle checkpoint that monitors kinetochore–microtubule attachment has been implicated in tumorigenesis; however, the relation between the spindle checkpoint and cell death remains obscure. In BUB1-deficient (but not MAD2-deficient) cells, conditions that activate the spindle checkpoint (i.e., cold shock or treatment with nocodazole, paclitaxel, or 17-AAG) induced DNA fragmentation during early mitosis. This mitotic cell death was independent of caspase activation; therefore, we named it caspase-independent mitotic death (CIMD). CIMD depends on p73, a homologue of p53, but not on p53. CIMD also depends on apoptosis-inducing factor and endonuclease G, which are effectors of caspase-independent cell death. Treatment with nocodazole, paclitaxel, or 17-AAG induced CIMD in cell lines derived from colon tumors with chromosome instability, but not in cells from colon tumors with microsatellite instability. This result was due to low BUB1 expression in the former cell lines. When BUB1 is completely depleted, aneuploidy rather than CIMD occurs. These results suggest that cells prone to substantial chromosome missegregation might be eliminated via CIMD.

Introduction

Defects in the attachment of microtubules to kinetochores activate the spindle checkpoint to delay mitotic progression by transiently inhibiting the anaphase-promoting complex (also called the cyclosome) (Rieder and Maiato, 2004). Genes involved in the spindle checkpoint were first isolated from *Saccharomyces cerevisiae* and include *MAD1*, *MAD2*, and *MAD3* (mitotic arrest–deficient) (Li and Murray, 1991); *BUB1*, *BUB2*, and *BUB3* (budding uninhibited by benzimidazole [a microtubule-depolymerizing drug]) (Hoyt et al., 1991); and *MPS1* (monopolar spindle) (Wells and Murray, 1996).

The spindle checkpoint proteins and their functions are highly conserved between yeast and humans, and defects in the spindle checkpoint result in substantial aneuploidy (Kitagawa and Hieter, 2001; Kops et al., 2005). Much evidence also indicates a role of the spindle checkpoint in tumorigenesis, e.g., mutations in human homologues of Bub1 (BUB1 and BUBR1) have been found in subtypes of colorectal cancer cells that exhibit chromosome instability (CIN) (Cahill et al., 1998). The CIN phenotype has been associated with mutations in spindle checkpoint genes (Ohshima et al., 2000; Tsukasaki et al., 2001; Ru et al., 2002), decreased levels of spindle checkpoint proteins (Shigeishi et al., 2001; Saeki et al., 2002), and loss of spindle checkpoint activity (Wang et al., 2002; Yoon et al., 2002). *Mad2*$^{+/-}$ mice frequently develop lung tumors after a long latency (Michel et al., 2001). *Bubr1*$^{+/-}$ mice and *Bub3*/*Rae1* heterozygotes are prone to tumor development (Babu et al., 2003; Dai et al., 2004). These results strongly suggest a close relation between altered activity of the spindle checkpoint and tumorigenesis. Also, many tumor cells have a diminished, but not absent, spindle checkpoint response (Kops et al., 2005).

When the function of mouse Bub1 is compromised cells appear to escape apoptosis and continue to progress through the cell cycle, despite leaving mitosis with an altered spindle (Taylor and McKeon, 1997). However, opposing evidence indicates that the spindle checkpoint regulates apoptosis: mutations in *bub1* cause chromosome missegregation and fail to block apoptosis in *Drosophila* (Basu et al., 1999), and *Mad2*-null mouse embryos undergo apoptosis at embryonic day (E) 6.5 to E7.5 (Dobles et al., 2000). In all of these cases, apoptosis appeared to occur in the subsequent G1 phase; thus, the role of the spindle checkpoint in apoptosis remained unclear.

When cells cannot satisfy the spindle checkpoint after a long mitotic delay, several cell fates can occur: some cells die during mitosis, some exit mitosis but die via apoptosis in the

Correspondence to Katsumi Kitagawa: katsumi.kitagawa@stjude.org

Abbreviations used in this paper: AIF, apoptosis-inducing factor; CIMD, caspase-independent mitotic death; CIN, chromosome instability; EndoG, endonuclease G; MIN, microsatellite instability; siRNA, small interfering RNA; TEM, transmission electron microscopy.

The online version of this article contains supplemental material.

The Journal of Cell Biology, Vol. 178, No. 2, July 16, 2007 283–296
http://www.jcb.org/cgi/doi/10.1083/jcb.200702134

G1 phase, and some exit mitosis but are tetraploid and reproductively dead (Rieder and Maiato, 2004). Microtubule inhibitors induce mitotic arrest by activating the spindle checkpoint; eventually, these inhibitors cause cytotoxicity. The cytotoxicity of microtubule inhibitors and resultant cell death has been described as either apoptosis in G1 or reproductive death (Mollinedo and Gajate, 2003). However, questions about cell death during mitosis have remained. Although much evidence suggests that apoptosis occurs during mitosis (Woods et al., 1995; DeLuca et al., 2002; Burns et al., 2003; Yang et al., 2005; Blank et al., 2006), in-depth analyses of mitotic cell death have not been performed; therefore, the mechanism involved remains obscure, especially the relation between the spindle checkpoint and cell death during mitosis. Here, we report the mechanism of the programmed cell death in early mitosis that is induced by defects in the kinetochore–microtubule attachment in BUB1-deficient cells.

Results

Substantial BUB1 depletion does not affect mitotic delay induced by defects in kinetochore–microtubule attachment

Treatment with nocodazole (a microtubule-depolymerizing drug), paclitaxel (Taxol, a microtubule-stabilizing drug) (Mollinedo and Gajate, 2003), or 17-allylaminogeldanamycin (17-AAG, an HSP90 inhibitor that induces delocalization of several kinetochore proteins from kinetochores) (Niikura et al., 2006) caused substantial mitotic delay (Fig. 1 A). We depleted HeLa cells of either BUB1 or MAD2 (both are spindle checkpoint components) by treating the cells with synthetic small interfering RNA (siRNA) (Fig. 1 B). The cells were then incubated in nocodazole, paclitaxel, or 17-AAG to induce mitotic arrest. The depletion of MAD2 (but not BUB1) substantially diminished the arrest (Fig. 1 A). These results are consistent with the finding by Johnson et al. (2004), i.e., depletion of BUB1 does not compromise the mitotic delay either during normal mitosis or in response to spindle damage induced by nocodazole (Johnson et al., 2004). Although a small remaining quantity of BUB1 may be sufficient to induce mitotic delay (Meraldi and Sorger, 2005), ~90% depletion of BUB1 did not affect mitotic delay induced by defects in kinetochore–microtubule attachment.

Depletion of BUB1 or MAD2 sensitizes cells to 17-AAG or paclitaxel

Synthetic lethality occurs between spindle checkpoint mutants and kinetochore mutants in yeast, presumably because of synergistic, substantial chromosome loss (Hyland et al., 1999; Tong et al., 2001). In human cells, simultaneous depletion of the kinetochore protein HEC1 and MAD2 causes premature catastrophic exit from mitosis (Martin-Lluesma et al., 2002). Because 17-AAG causes kinetochore defects (Niikura et al., 2006), we examined whether 17-AAG treatment in conjunction with defects in the spindle checkpoint induces synthetic lethality. MAD2 or BUB1 was depleted from HeLa cells by siRNA treatment. The cells were then exposed to 100 nM 17-AAG, which did not kill most control cells, and viability was evaluated by a colony outgrowth assay (Fig. 1 C, top). The proportion of cells killed by MAD2 siRNA or BUB1 siRNA alone did not differ from that seen with control luciferase siRNA, but treatment with either MAD2 siRNA or BUB1 siRNA and 17-AAG caused substantial synergistic lethality (Fig. 1 C).

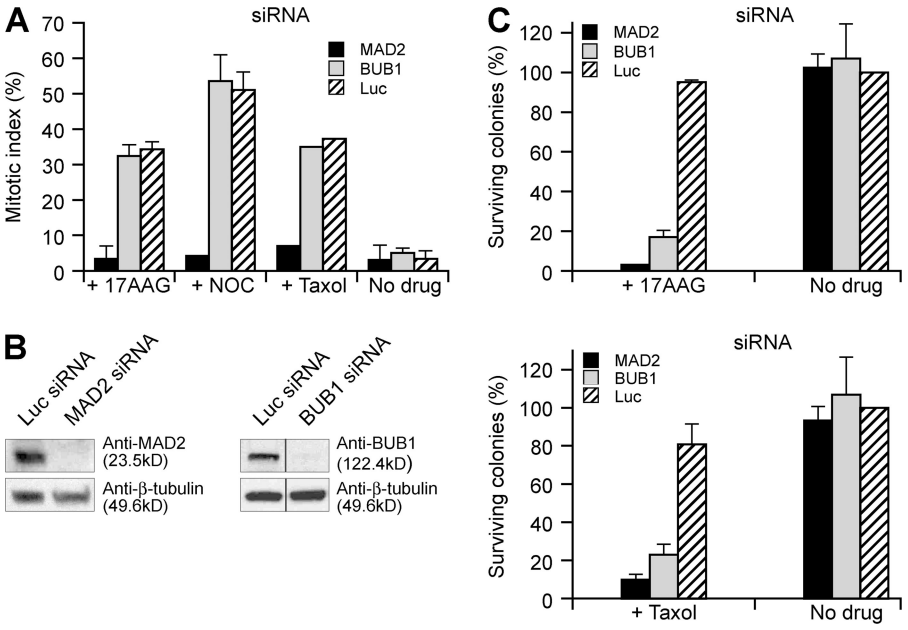

Figure 1. **Mitotic delay induced by defects in kinetochore-microtubule attachment was not affected by substantial depletion of BUB1.** (A) The proportion of cells in mitotic arrest caused by 17-AAG (+17AAG), nocodazole (+NOC), or paclitaxel (+Taxol) was reduced by MAD2 siRNA, but not by BUB1 siRNA. We added 17-AAG (500 nM), NOC (0.5 μg/ml), or Taxol (10 nM) 48 h after transfection with MAD2 siRNA, BUB1 siRNA, or luciferase (Luc) siRNA, and the cells were incubated for 24 h. Cells were fixed, stained with DAPI, and subjected to fluorescence microscopy. The mean percentages (± SD) of cells in prophase, prometaphase, or metaphase are shown, as determined by analyzying 500 cells in three independent experiments. (B) Western blot analysis of total HeLa cell lysates harvested 48 h after transfection with siRNA duplexes directed against MAD2 (left) and BUB1 (right) revealed protein depletion. Luc siRNA was transfected into the cells as a control. The level of β-tubulin protein was used as a loading control. (C) Depletion of MAD2 or BUB1 sensitizes cells to 17-AAG (top) and Taxol (bottom). Colony outgrowth assays of HeLa cells transfected with siRNAs against MAD2, BUB1, or Luc. We normalized the percent viability; the percentage of surviving colonies in control wells (Luc siRNA and no drug) was set to 100. Three independent experiments were performed for each drug.

Spindle checkpoint mutants in yeast are also sensitive to microtubule inhibitors (Hoyt et al., 1991; Li and Murray, 1991), presumably because of synergistic substantial chromosome loss. Therefore, we examined whether paclitaxel treatment, in conjunction with defects in the spindle checkpoint, induces synthetic lethality. Like 17-AAG, paclitaxel with either MAD2 siRNA or BUB1 siRNA caused substantial synergistic lethality (Fig. 1 C). Death induced by MAD2 siRNA and 17-AAG or paclitaxel is presumably caused by the failure of checkpoint-induced mitotic arrest, which results in premature mitotic exit and synergistic aneuploidy (Fig. 2 A). The resulting abnormal nuclei (i.e., fragmented/aggregated nuclei, micronuclei, or chromosome bridges; Fig. 2 B) are similar to those of cells that are MAD2 depleted for several cell divisions (Kops et al., 2004); this lethal phenotype can be explained by premature mitotic exit, i.e., the current understanding of how the spindle checkpoint protects cells from aneuploidy (Mollinedo and Gajate, 2003) (Fig. 2 A). Moreover, the abnormal nuclear phenotypes are associated with the degree of MAD2 depletion (Fig. 2, C and D). However, BUB1-depleted cells treated with 17-AAG or paclitaxel did not appear to exit mitosis (Fig. 1 A). This finding raises a provoking question: How does simultaneous treatment with BUB1 siRNA and 17-AAG or paclitaxel cause substantial synergistic lethality, when BUB1 depletion does not cause premature mitotic exit? The spindle checkpoint appeared functional (Fig. 3 A).

Microtubule inhibitors or 17-AAG induce mitotic cell death in BUB1-depleted cells

To evaluate the lethal phenotype caused by 17-AAG and either MAD2 siRNA or BUB1 siRNA, we used the TUNEL assay. When cells were treated simultaneously with 17-AAG and BUB1 siRNA, but not with MAD2 siRNA, most of the TUNEL$^+$ cells were in prophase, prometaphase, or metaphase (Fig. 3, B and C). Furthermore, agarose gel electrophoresis directly detected DNA fragmentation in the mitotic cells (Fig. 3 E).

To exclude the possibility of off-targets of siRNA, we used several siRNA oligos to induce DNA fragmentation (unpublished data; see Fig. S4 A, available at http://www.jcb.org/cgi/content/full/jcb.200702134/DC1). Overexpression of BUB1 suppressed DNA fragmentation when siRNA targeted the 3′ UTR region of BUB1 (Fig. S1, A and B). Although the BUB1-depleted cells appeared to be arrested in mitosis, they must have been dead or dying, because the DNA had already fragmented

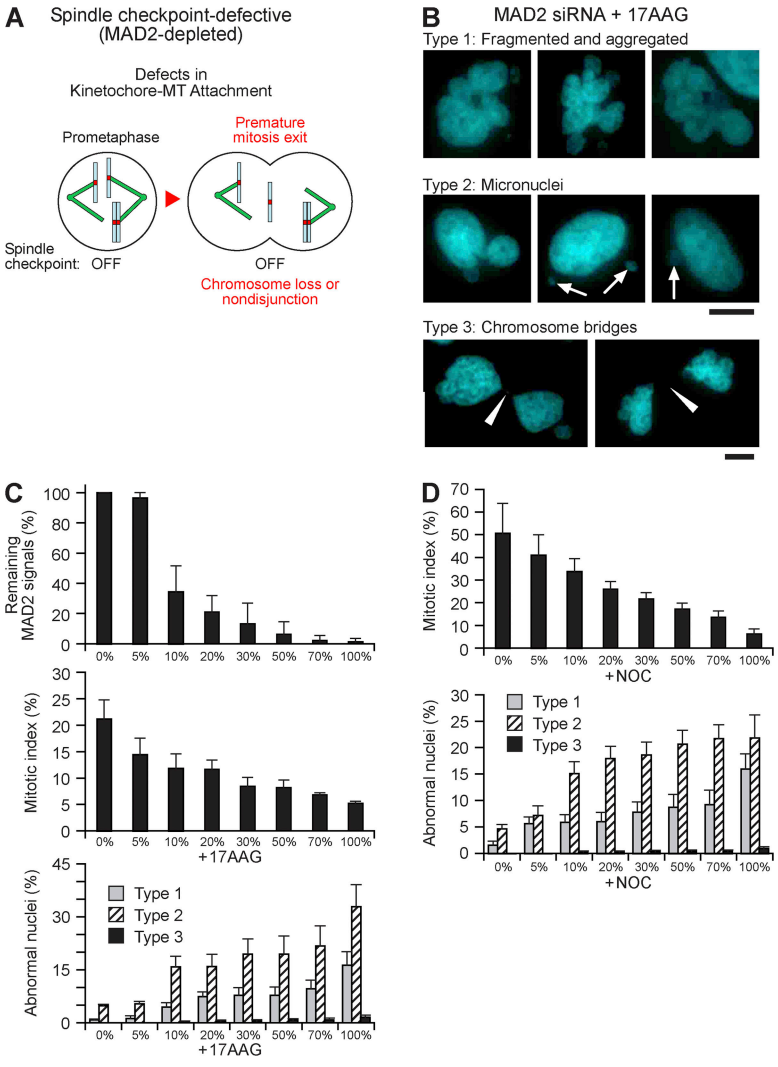

Figure 2. **MAD2 depletion causes premature exit from mitosis.** (A) A model showing how chromosome loss or nondisjunction occurs in spindle checkpoint–defective cells. In spindle checkpoint mutant cells, the spindle checkpoint is not activated, even if kinetochore–microtubule attachment is defective. No mitotic delay occurs, and premature exit from mitosis results. Thus, substantial chromosome loss or nondisjunction occurs and presumably cell death will follow. (B) MAD2-depleted and 17-AAG–treated cells have abnormal nuclei. After 48 h of transfection with MAD2 siRNA, HeLa cells were incubated with 17-AAG (500 nM) for 24 h at 37°C. Cells were fixed, and DNA was visualized by staining with DAPI (blue). Type 1 refers to fragmented and aggregated nuclei; type 2, to micronuclei (arrows); and type 3, to chromosome bridges (arrowheads). Bars, 10 µm. (C) The siRNA dilution experiment using MAD2 targets that deplete MAD2 almost completely. (Top) Quantified MAD2 expression levels are shown. The X-axis indicates dilutions of MAD2 siRNA oligos. The Y-axis indicates the remaining MAD2 signals. (Middle) The mitotic index induced by 17-AAG is reduced as MAD2 is depleted. (Bottom) The number of 17-AAG–induced abnormal nuclei also increased in proportion as MAD2 is depleted. (D, top) The mitotic index induced by NOC is reduced as MAD2 is depleted. (bottom) The number of NOC-induced abnormal nuclei also increased in proportion as MAD2 is depleted.

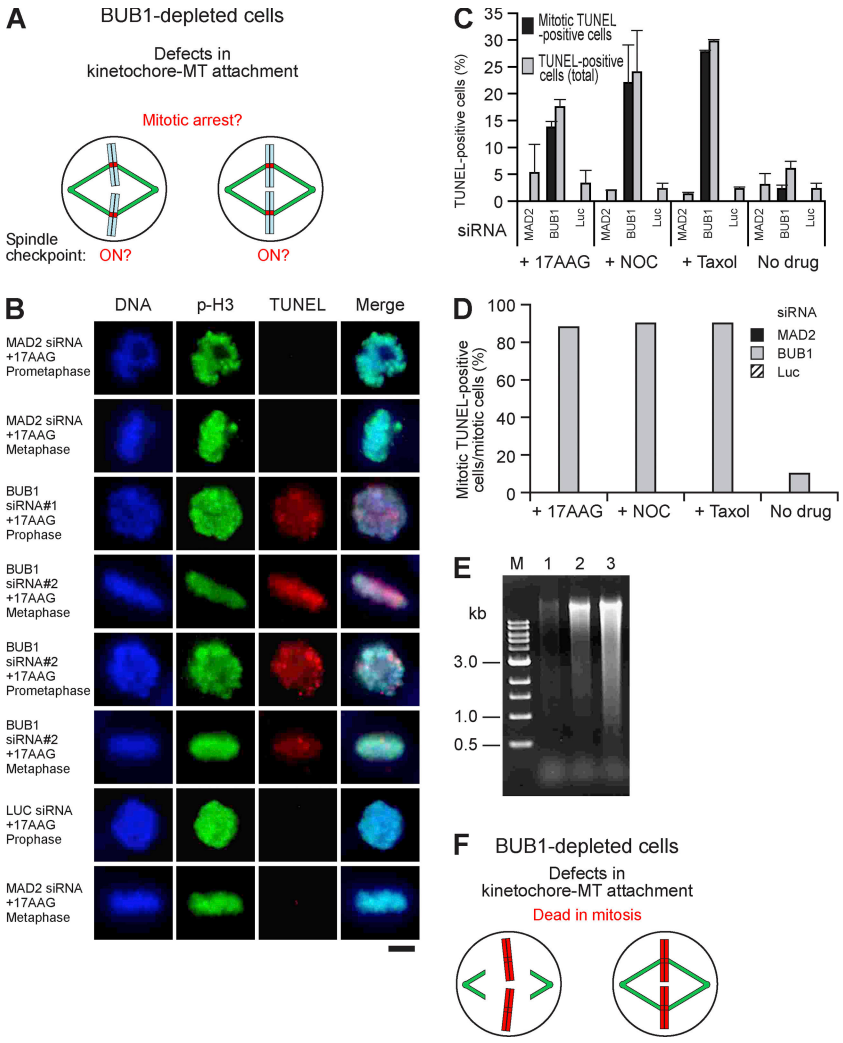

Figure 3. **CIMD occurs in BUB1-depleted cells in the presence of microtubule inhibitors or 17-AAG.** (A) A model showing BUB1-depleted cells. When cells had defective kinetochore–microtubule attachment, mitotic delay occurred, and the spindle checkpoint appeared to be active (ON). The substantial synthetic lethality cannot be explained because there is no premature exit from mitosis. (B) HeLa cells that are BUB1-depleted and 17-AAG–treated exhibit DNA fragmentation (TUNEL$^+$) during mitosis. 48 h after HeLa cells were transfected with siRNA against MAD2, BUB1, or Luc, they were incubated with 17-AAG (+17AAG, 500 nM) for 24 h at 37°C. Fixed samples were stained by using an in situ cell death detection system that contained TMR red (red), an anti-phosphorylated histone H3 (p-H3) mouse monoclonal antibody, and FITC-conjugated secondary antibodies (green). DNA was stained with DAPI (blue) to visualize prophase, prometaphase, and metaphase cells. Bar, 10 μm. (C) A histogram summarizing TUNEL assay results of BUB1- or MAD2-depleted cells. HeLa cells transfected with siRNA against MAD2, BUB1, or Luc were treated with 17-AAG (500 nM), NOC (0.5 μg/ml), or Taxol (10 nM) for 24 h at 37°C. DNA fragmentation was detected by the TUNEL assay, and samples underwent indirect fluorescence microscopy using anti–p-H3 as a primary antibody. More than 200 cells in three independent experiments were counted, and the mean percentages (± SD) of TUNEL$^+$ cells and mitotic TUNEL$^+$ cells (mitotic cells were those that were positive for p-H3 and had characteristic chromosome morphology) were calculated. Gray bars represent the mean percentages of TUNEL$^+$ cells in the population, and black bars indicate the mean percentages of mitotic TUNEL$^+$ cells. (D) Almost 90% of the BUB1-depleted mitotic cells that were treated with 17-AAG, NOC, or Taxol were TUNEL$^+$. A histogram summarizing TUNEL assay results of 17-AAG-treated and BUB1- or MAD2-depleted mitotic cells is shown in C. The number of TUNEL$^+$ cells among more than 200 mitotic cells was counted, and the percentages (i.e., the number of mitotic TUNEL$^+$ cells per that of total mitotic cells) are shown. MAD2 or Luc siRNA did not induce any mitotic TUNEL$^+$ cells. (E) DNA fragmentation in BUB1-depleted and 17-AAG–treated mitotic HeLa cells was detected by electrophoresis. 48 h after HeLa cells were transfected with BUB1 siRNA, they were treated with 17-AAG (500 nM) for 6 h. Mitotic cells were isolated by pipetting (~90% of the isolated population consisted of mitotic cells), and DNA was extracted and subjected to electrophoresis in a 1% agarose gel (lane 2). As a negative control, DNA extracted from mitotic HeLa cells treated with 17-AAG (500 nM) was loaded (lane 1); and as a positive control, we loaded DNA extracted from HeLa cells treated with staurosporine (1 μM), a known inducer of apoptosis (lane 3). The molecular size markers (1-kb DNA ladder; New England Biolabs) are indicated (lane M). Fragmented DNA prepared from the same amount of cells was loaded into each lane. Our method of DNA isolation isolated only fragmented DNA; therefore, if cells contained little or no fragmented DNA, the same was observed in that lane. (F) A model showing BUB1-depleted cells in which defects in kinetochore–microtubule attachment induce lethal DNA fragmentation. Because cells are still arrested in mitosis, the mitotic index is unchanged. Therefore, the spindle checkpoint appears to be active (ON).

during early mitosis (Fig. 3 F). This finding answers the question posed above.

Cells treated with BUB1 siRNA and either nocodazole or paclitaxel underwent mitotic cell death (Fig. 3 C; Fig. S1 C). Interestingly, ~90% of the mitotic cells were TUNEL$^+$ (Fig. 3 D). These drugs commonly cause defective kinetochore–microtubule attachment. Therefore, these results strongly suggest that this mitotic cell death occurs when the kinetochore–microtubule attachment is altered and BUB1 function is disrupted.

Caspase-independent mitotic death

We detected no caspase activity (caspases 1, 3–9) in cells exposed to 17-AAG and BUB1 siRNA (Fig. 4 A). Furthermore, caspase inhibitors BAF and zVAD did not inhibit DNA fragmentation induced by 17-AAG and BUB1 siRNA (Fig. 4 B, see Fig. S1 D for drug evaluation controls). Therefore, this mitotic cell death was caspase independent. Apoptosis caused by spindle checkpoint defects is thought to occur during the G1 phase, and the type of cell death that we identified does not meet the criteria for other defined types of cell death (Okada and Mak, 2004); thus, we designated this type of cell death as caspase-independent mitotic death (CIMD).

Because CIMD occurs in HeLa cells with compromised p53 activity (Hoppe-Seyler and Butz, 1993), CIMD appeared to be independent of p53. We confirmed that CIMD occurs in cells that lack p53 (Figs. 4 C; Fig. S1 E and Table S1). Next, we examined whether CIMD depends on p73, a homologue of p53, because a mitotic function of p73 has been suggested (Fulco et al., 2003; Merlo et al., 2005). Overexpression of the dominant-negative mutant p73DD (Irwin et al., 2000) suppressed CIMD

(Figs. 4 D; Fig. S1 F), depletion of p73 diminished CIMD (Fig. 4 E), and CIMD did not occur efficiently in $p73^{-/-}$ MEF cells (Irwin et al., 2000) (Fig. S2 A, available at http://www.jcb.org/cgi/content/full/jcb.200702134/DC1). These results indicate that CIMD depends on p73 but not on p53.

Mitochondria release apoptosis-inducing factor (AIF) and endonuclease G (EndoG) (Susin et al., 1999; Li and Hoffman, 2001; van Loo et al., 2002), which are thought to regulate caspase-independent cell death (Susin et al., 2000; Joza et al., 2001; Cregan et al., 2002; Yu et al., 2002). Therefore, we examined whether AIF and EndoG are required for CIMD. Substantial amounts of AIF and EndoG were released from mitochondria in mitotic cells treated with 17-AAG and BUB1 siRNA (Fig. 5, A and C). AIF and EndoG immunostaining resulted in a pattern that resembled that of mitochondria stained with 3,3′-dihexyloxacarbocyanine iodide ($DiOC_6$) in mitotic cells, as described previously (Barni et al., 1996). We confirmed that AIF and EndoG immunostaining was colocalized with MitoTracker Red CM-HsXRos staining (Fig. S2 B). The proportion of AIF- and EndoG-releasing mitotic cells was comparable to that of cells undergoing CIMD (compare Fig. 5, B and D with Fig. 4 B); this similarity strongly suggests that AIF and EndoG are effectors of CIMD.

Next, we examined whether CIMD depends on AIF and EndoG. Depletion of AIF and EndoG by siRNA treatment substantially reduced TUNEL signals that were induced by 17-AAG treatment and BUB1 depletion (Fig. 5 E; Fig. S2 C), whereas depletion of AIF, EndoG, or both did not affect the mitotic delay induced by 17-AAG (Fig. S2 D). These results indicate that DNA fragmentation is dependent on AIF and EndoG.

We examined whether depletion of EndoG and AIF rescues the lethality caused by CIMD. Although depletion of AIF or EndoG alone did not rescue the lethality, of both EndoG and AIF substantially suppressed it (Fig. 5 F), indicating that both effectors are involved in the death-signaling pathway of CIMD. These findings lead us to conclude that CIMD is an active cell death system mediated by these apoptosis effectors.

CIMD occurs rapidly after the kinetochore–microtubule attachment is altered

Inhibition of DNA decatenation arrests cells at metaphase, and the disruption of MAD2, but not BUB1, suppresses this metaphase arrest (Skoufias et al., 2004). Therefore, we examined whether CIMD occurs when BUB1-depleted cells are arrested with ICRF187, a topoisomerase II inhibitor. Although we observed a substantial mitotic delay after ICRF187 treatment (unpublished data), the number of $TUNEL^+$ BUB1-depleted cells was unchanged (Fig. S2 E). This finding suggests that inhibition of DNA decatenation does not induce CIMD and supports the hypothesis that CIMD occurs specifically when the kinetochore–microtubule attachment is altered.

To investigate the timing of CIMD after the kinetochore–microtubule attachment is altered, we added 17-AAG or microtubule inhibitors to BUB1-depleted cells that were arrested by ICRF187. We then monitored $TUNEL^+$ cells. CIMD began to occur within 20 min, and most of the mitotic cells were $TUNEL^+$ within 2 h (Fig. 6 A). This finding indicates that CIMD occurs during mitosis and relatively rapidly after the kinetochore–microtubule attachment is altered, which supports our conclusion that CIMD is an active cell death system.

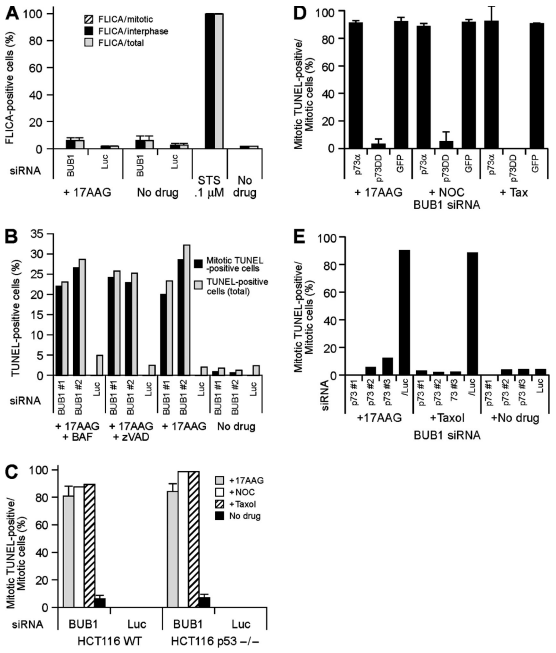

Figure 4. **CIMD is independent of caspase and p53 but dependent on p73.** (A) Mitotic cell death induced by BUB1 siRNA and 17-AAG treatment did not activate caspases. 48 h after transfection of HeLa cells with BUB1 or Luc siRNA, they were incubated with 17-AAG (500 nM) for 24 h at 37°C. As a positive control, HeLa cells were treated with 1 μM staurosporine (STS) for 6 h. Cells were incubated in the FAM-VAD-FMK FLICA (fluorochrome inhibitor of caspases) solution (Immunochemistry Technologies, LLC) for 60 min at 37°C to detect activated caspases 1, and 3–9. Samples were examined under a fluorescent microscope, and the number of $FLICA^+$ cells among more than 200 cells was counted. The calculated percentages are shown. Black bars represent the mean percentages (± SD) of interphase $FLICA^+$ cells, whereas gray bars indicate the mean percentage (± SD) of all cells that were $FLICA^+$. No mitotic $FLICA^+$ (striped bars) were observed. (B) Pan-caspase inhibitors VAD (zVAD; 50 μM) or BAF (50 μM) did not suppress mitotic cell death induced by BUB1 siRNA and 17-AAG treatment. Black bars represent the mean percentages (± SD) of mitotic $TUNEL^+$ cells, whereas gray bars indicate the mean percentage (± SD) of all $TUNEL^+$ cells. Pan-caspase inhibitors zVAD (50 μM) or BAF (50 μM) were applied 1 h before 17-AAG treatment, and they remained in the medium during 17-AAG treatment. (C) CIMD is independent of p53. DNA fragmentation that was caused by BUB1 depletion and treatment with 17-AAG or microtubule inhibitors occurred in $p53^-$ cells, i.e., HCT116-$p53^{-/-}$ cells. (D) Overexpression of the dominant-negative mutant p73DD can suppress CIMD. We transfected HeLa cells with p73a plasmid, p73DD plasmid, or GFP vector only. At 48 h after transfection, we treated cells with 17-AAG, NOC, or Taxol and incubated them for 24 h. Cells were fixed, and only GFP^+ cells were detected under a microscope. (E) DNA fragmentation induced by BUB1 siRNA and 17-AAG or Taxol treatment was suppressed when p73 was depleted. HeLa cells were cotransfected with siRNA against BUB1 and Luc or BUB1 and one of three siRNAs against p73 (#1, #2, or #3). 48 h later, the cells were incubated with 17-AAG (500 nM) for 24 h at 37°C. Fixed samples were stained by using an in situ cell death detection system.

To investigate the timing of CIMD after the kinetochore–microtubule attachment is altered, we added 17-AAG or microtubule inhibitors to BUB1-depleted cells that were arrested by ICRF187. We then monitored $TUNEL^+$ cells. CIMD began to occur within 20 min, and most of the mitotic cells were $TUNEL^+$ within 2 h (Fig. 6 A). This finding indicates that CIMD occurs during mitosis and relatively rapidly after the kinetochore–microtubule attachment is altered, which supports our conclusion that CIMD is an active cell death system.

We also tested whether cold shock induces CIMD. Cold treatment depolymerizes microtubules, which activates the spindle checkpoint (Rieder and Cole, 2002). When cells were incubated at 23°C, CIMD occurred in >90% of the mitotic cells within 3 h (Fig. 6 B). This is the fourth piece of evidence that supports the hypothesis that CIMD is caused by defects in kinetochore–microtubule attachment when BUB1 function is disrupted.

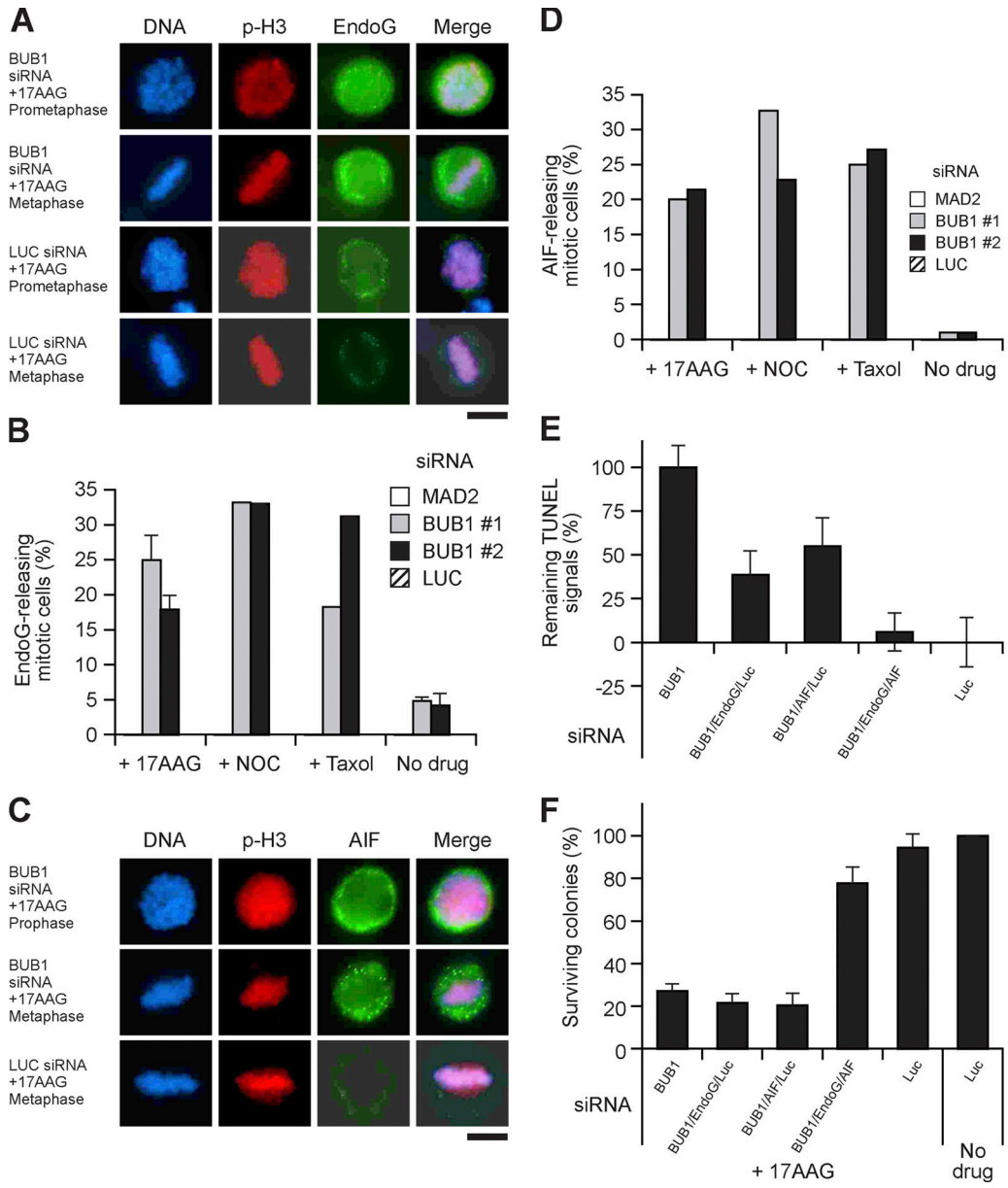

Figure 5. **CIMD is dependent on EndoG and AIF.** (A) BUB1 siRNA and 17-AAG treatment release EndoG from mitochondria of mitotic cells. Fixed cells were stained using anti-EndoG rabbit polyclonal antibody and anti–p-H3 mouse monoclonal antibody as primary antibodies. FITC- and Texas red–conjugated secondary antibodies (green and red signals, respectively) were added to visualize specific proteins. DNA was stained with DAPI (blue). Samples were analyzed by fluorescence microscopy, and images were captured. Bar, 10 μm. (B) HeLa cells transfected with MAD2 siRNA, BUB1 siRNA #1, BUB1 siRNA #2, or Luc siRNA were treated with 17-AAG (500 nM), NOC (0.5 μg/ml), or Taxol (10 nM) for 24 h at 37°C. The number of mitotic EndoG-releasing cells was counted among more than 200 cells; mitotic cells were those that were p-H3$^+$ and had characteristic chromosome morphology. The mean percentages (± SD) are shown. EndoG was not released in cells treated with siRNA against MAD2 or Luc. (C) An anti–apoptosis-inducing factor (AIF; green) rabbit polyclonal antibody was used to detect the release of AIF from mitochondria in response to BUB1 siRNA and 17-AAG treatment. Bar, 10 μm. (D) Bars represent the percentages of the mitotic AIF-releasing cells (i.e., cells positive for AIF release p-H3 and mitotic condensed chromosomes). AIF was not released from cells treated with siRNAs against MAD2 or Luc. (E) DNA fragmentation induced by BUB1 siRNA and 17-AAG treatment was suppressed when EndoG and AIF were depleted. HeLa cells were cotransfected with BUB1 siRNA and Luc siRNA; BUB1 siRNA and EndoG siRNA; BUB1 siRNA and AIF siRNA; or Luc siRNA. 48 h later, the cells were incubated with 17-AAG (500 nM) for 24 h at 37°C. Fixed samples were stained using an in situ cell death detection system, and TUNEL signals (black bars) were quantified by using Openlab version 4.0.4. Scientific Imaging Software (Improvision). (F) Depletion of EndoG and AIF rescues the lethality of cells treated with 17-AAG and BUB1 siRNA. Results from colony outgrowth assays of HeLa cells transfected with siRNAs directed against the indicated proteins are shown. We normalized the percent viability; the percentage of surviving colonies in control wells (Luc siRNA and no drug) was set to 100. Three independent experiments were performed.

The fate of cells in which CIMD occurred

To learn the fate of cells in which DNA was fragmented during mitosis, we performed time-lapse experiments. Most BUB1-depleted cells that remained in mitosis for ∼6 h after the addition of 17-AAG eventually collapsed directly from mitosis within 12 h (Fig. 6, C–E). In contrast, most luciferase siRNA–treated cells (a negative control) remained in mitosis up to 12 h later (Fig. 6, C and D). Therefore, the cells in which CIMD occurred looked

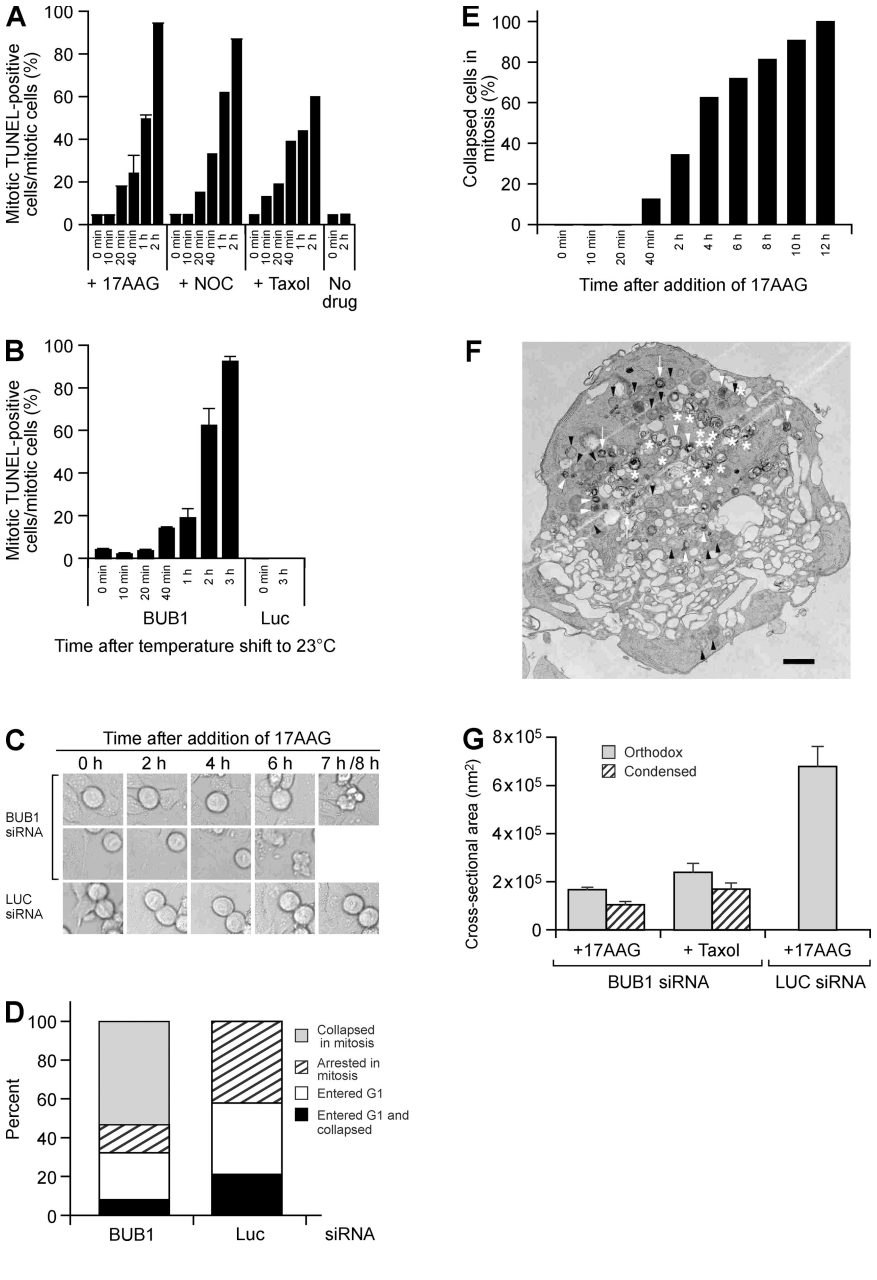

Figure 6. **CIMD occurs rapidly after defects in kinetochore–microtubule attachment occur.** (A) 48 h after HeLa cells were transfected with BUB1 siRNA, they were incubated with ICRF187 (1 mM) for 6 h at 37°C. Mitotic cells were collected, and 17-AAG, NOC, or Taxol was added. TUNEL assays were performed at 0, 10, 20, and 40 min, and 1, and 2 h after the addition of 17-AAG, NOC, or Taxol. (B) 48 h after HeLa cells were transfected with BUB1 siRNA, they were incubated with ICRF187 (1 mM) for 6 h at 37°C. Mitotic cells were collected, and the temperature was shifted from 37 to 23°C. TUNEL assays were performed at 0, 10, 20, and 40 min, and 1, 2, and 3 h after the temperature shift. (C) Live-image analysis of BUB1-depleted cells after treatment with 17-AAG. Phase-contrast images were taken at the indicated time points after addition of 17-AAG. (Top and middle) Examples of BUB1-depleted cells that collapsed during mitosis. (Bottom) Examples of Luc siRNA–treated cells arrested in mitosis for 8 h. (D) The fate of the cells in which CIMD occurred. The morphologic phenotypes that were observed for 12 h after addition of 17-AAG were categorized into four types: those that collapsed during mitosis (gray), those that arrested in mitosis (striped), those that entered G1 (white), and those that entered G1 and collapsed (black). (E) Time course of mitotic collapse within 12 h after addition of 17-AAG. Bars indicate the percentages of the mitotic cells that collapsed at the indicated time points out of the mitotic cells that eventually collapsed. (F) Electron microscopy images of BUB1-depleted cells that were treated with 17-AAG for 3 h. Orthodox or swollen mitochondria (black arrowheads), condensed mitochondria (white arrowheads), whorls or onion-skin mitochondria (white arrows), and autophagosomes (asterisks) are indicated. Bar, 1 μm. (G) Histogram of mitochondrial cross-sectional areas in images of treated and control cells. The cross-sectional area, measured with the program ImageJ, is an estimate of the volume of the mitochondria. Mitochondria were classified according to orthodox and condensed morphology. The condensed mitochondria not only had a condensed matrix but also were smaller than the orthodox mitochondria in the same cells. The control (17AAG_Luc siRNA) samples had orthodox but few condensed mitochondria, hence the cross-sectional area was measured for only the orthodox mitochondria. Both the 17AAG_BUBsiRNA and Tax_BUBsiRNA cross-sectional areas were ~3 times less than the control, suggesting that fission of the mitochondria occurred. Error bars represent the SEM. The value over the error bar is the number of mitochondria measured per condition.

normally arrested in mitosis for several hours after the kinetochore–microtubule attachment was altered.

Most conventional apoptosis detection methods (i.e., annexin V assay, chromatin condensation, and other morphologic analyses by light microscopy) were not applicable to mitotic cells (unpublished data). Therefore, we performed transmission electron microscopy (TEM) to look at the ultrastructural features of cells in which CIMD had occurred. When DNA fragmentation was induced by BUB1 depletion and 17-AAG or paclitaxel, we observed increased numbers of abnormal mitochondria (condensed, whorled, or onion-skin) and autophagosomes (Fig. 6 F; Fig. S3, A and C, available at http://www.jcb.org/cgi/content/full/jcb.200702134/DC1). The mitochondria were significantly smaller than those in control cells (Fig. 6 G), suggesting that mitochondrial fragmentation occurred. These changes indicated active cell death, possibly through autophagy (Perkins et al., 2004; Eskelinen, 2005; Barsoum et al., 2006; Perez et al., 2007).

Partial, but not complete, depletion of BUB1 causes CIMD

BUB1 depletion does not compromise mitotic delay during normal mitosis or in response to nocodazole-induced spindle damage (Johnson et al., 2004). Our findings support that earlier study, and we believe that we can now explain this phenomenon. Because CIMD occurred, the mitotic index appeared to be unchanged. When a small amount of BUB1 remains in the cell

it is sufficient to induce mitotic delay, but when BUB1 is completely depleted, cells prematurely exit mitosis (Meraldi and Sorger, 2005). Therefore, we attempted to determine how much BUB1 would have to be depleted to induce CIMD.

We performed an siRNA dilution experiment using BUB1 targets to deplete BUB1 almost completely. When BUB1 was nearly depleted, CIMD occurred or the mitotic index was significantly reduced (Fig. 7, A and B; Fig. S4 A, available at http://www.jcb.org/cgi/content/full/jcb.200702134/DC1). Therefore, complete depletion of BUB1 causes premature mitotic exit. The number of abnormal nuclei was also increased similarly to that seen after MAD2 depletion (Fig. 7 C), and partial depletion of MAD2 did not induce CIMD (Fig. 2; Fig. S4 B).

These results indicate that CIMD does not occur when BUB1 is almost completely depleted; the remaining BUB1 appears to be required to induce CIMD. A substantial number of cells with abnormal nuclei did not result from CIMD, which raises the possibility that CIMD might kill the cells that are going to have abnormal nuclei. Furthermore, a kinase-dead BUB1 mutant failed to suppress CIMD, which suggests that the kinase activity is important for inhibition of CIMD (Fig. 7 D).

CIMD is a major cell death mechanism of tumors with CIN that is induced by microtubule inhibitors or 17-AAG

CIMD depends on BUB1 depletion, which suggests that microtubule inhibitors or 17-AAG induces CIMD of tumor cells that have a deficient spindle checkpoint. We tested whether microtubule inhibitors or 17-AAG induces CIMD of cells derived from tumors with CIN in which the spindle checkpoint is compromised and of tumor cells with microsatellite instability (MIN) in which the spindle checkpoint is intact (Cahill et al., 1998). CIMD occurred in tumor cell lines with CIN (Caco-2, SW480, and HT29) but not in those with MIN (SW38, DLD-1, and HCT116) (Fig. 7 E). CIMD occurred in 70–90% of the tumor cells with CIN that were $TUNEL^+$ (unpublished data).

We did not detect any caspase (caspases 1, 3–9) activity in mitotic tumor cells with CIN (Fig. S4 D), and caspase inhibitors BAF and zVAD did not inhibit DNA fragmentation (Fig. S4 E). These results suggest that the tumor cell lines with CIN have defective BUB1 pathways. In an early study, BUB1 mutations were not found in these cells (Cahill et al., 1998). Therefore, we measured the BUB1 protein levels in tumor cells with CIN; the level of BUB1 expression in tumors with CIN was lower than that in tumor cells with MIN or in HeLa cells (Fig. 7 F). The BUB1 levels in the tumor cells with CIN were ~40% of that in HeLa cells (Fig. S4 F). Partial reduction of BUB1 in HeLa cells can induce CIMD; therefore, the low level of BUB1 expression could explain why the tumors with CIN induce CIMD. To test this theory, we overexpressed BUB1 in tumor cells with CIN to see whether restoring BUB1 levels suppresses CIMD. As expected, overexpression of BUB1 suppressed CIMD in the colon tumor cell lines with CIN (Fig. 7 G; Fig. S1 B). Furthermore, the expression of the *Bub1* mutant allele Bub1*V400, which was found in a tumor cell with CIN, (Cahill et al., 1998) induced CIMD in HeLa cells (Fig. 7 H; Fig. S1 B). These findings suggest that CIMD is a main mechanism by which microtubule inhibitors and 17-AAG kill tumor cells with CIN.

Discussion

When the spindle checkpoint detects defects in the attachment of microtubules, it induces mitotic delay (Rieder and Maiato, 2004). The loss of the spindle checkpoint activity, especially in cells with chromosome segregation defects, is thought to result in aneuploidy. The apoptosis of aneuploid cells during the subsequent G1 phase may prevent tumorigenesis (Mollinedo and Gajate, 2003). We found that CIMD occurs in BUB1-deficient cells that have defects in kinetochore–microtubule attachment. When BUB1 is completely depleted, premature mitotic exit occurs rather than CIMD.

CIMD, mitotic catastrophe, and apoptosis

The combination of cell damage and deficient cell cycle checkpoints, in particular the DNA structure checkpoints and the spindle checkpoint, cause mitotic catastrophe (Castedo et al., 2004; Okada and Mak, 2004). Multinucleate and giant cells that contain uncondensed chromosomes form after mitotic catastrophe (Okada and Mak, 2004); these features obviously differ from those observed during CIMD and are rather similar to those observed in MAD2-depleted cells. Two types of mitotic catastrophe have been defined: in the first type, the cell dies in a p53-dependent manner during or near metaphase; in the second type, death occurs in a partially p53-dependent manner after failed mitosis and during the activation of the polyploidy checkpoint (Castedo et al., 2004). Mitotic catastrophe also is accompanied by chromatin condensation, mitochondrial release of proapoptotic proteins, caspase activation, and DNA degradation (Castedo et al., 2004). In contrast, CIMD occurs in a p53-independent manner. Furthermore, the spindle checkpoint is required for mitotic catastrophe induced by DNA-damaging agents (Nitta et al., 2004). Therefore, we conclude that the features of CIMD differ from those of mitotic catastrophe.

Several reports have described apoptosis during mitosis. High concentrations of paclitaxel (>25 nM for HeLa cells) are very cytotoxic (Woods et al., 1995). When 100–200 nM paclitaxel was used, p53-independent, $TUNEL^+$ cells appeared to be in prophase. The morphology of the $TUNEL^+$ cells also resembled that of cells undergoing apoptosis (i.e., the nuclei were bubble-shaped and fragmented); this appearance differs from that observed during CIMD. High concentrations of paclitaxel induce apoptosis by activating kinase pathways that include Akt and mTOR (Asnaghi et al., 2004). In our study, we used 10 nM paclitaxel at a low concentration (10 nM; see a comparison of the effects of different paclitaxel doses in Fig. S1 C) that was sufficient to cause substantial mitotic delay but did not induce apoptosis in most cells (Woods et al., 1995). Several hours after treatment with paclitaxel or nocodazole, 80% of Snk/Plk2-depleted $p53^+$ cells contain active caspase 3, and 4N cells are cyclin B^+ (Burns et al., 2003). Mitosin/CENP-F depletion induces premature chromosome decondensation followed by cell death with caspase activation (Yang et al., 2005).

Cells depleted of hNuf2 exit directly from prolonged mitotic arrest, exhibit apoptotic cell morphology, and contain DNA that resembles DNA in cells undergoing apoptosis (DeLuca et al., 2002). Because hNuf2 depletion blocks stable kinetochore–microtubule attachment, one could argue that hNuf2 depletion–induced cell

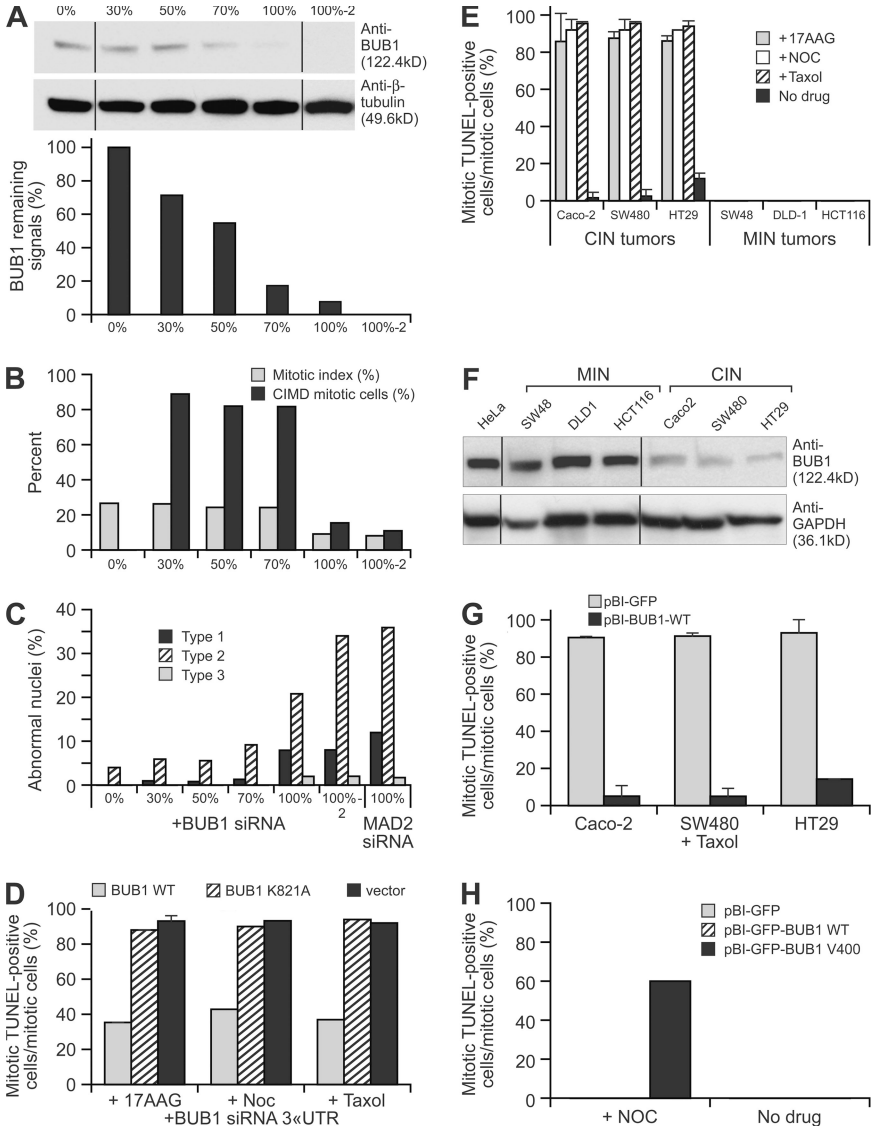

Figure 7. **Partial BUB1 depletion induces CIMD.** (A) The siRNA dilution experiment using BUB1 targets that deplete BUB1 almost completely. Percentages indicate dilutions, e.g., 100% means no dilution and 0% means no oligo was used. A different siRNA oligo set was used for 100%-2. (Top) Western blotting using anti-BUB1 antibody. (Bottom) Quantified BUB1 expression levels are shown. The X-axis indicates dilutions of BUB1 siRNA oligos. The Y-axis indicates the remaining BUB1 signals. (B) Mitotic index and mitotic TUNEL$^+$ cells (CIMD/mitotic cells) are shown. CIMD cells or the mitotic index is significantly reduced when BUB1 is depleted almost completely (100% and 100%-2). These data indicate that complete depletion of BUB1, like that of MAD2, causes premature mitotic exit. (C) The number of abnormal nuclei also increased to that seen after MAD2 depletion. (D) A kinase-dead BUB1 mutant failed to suppress CIMD. Ecotopic expression of wild-type (WT) BUB1 but not a kinase-dead mutant BUB1K821A (Cahill et al., 1998) suppresses CIMD when siRNA targets the 3′-UTR region of BUB1. (E) TUNEL assays were performed on three tumor cell lines with CIN (Caco-2, SW480, and HT29) and on three tumor cells lines with MIN (SW48, DLD-1, and HCT116) treated with 17-AAG (500 nM), NOC (0.5 mg/ml), or Taxol (10 nM) for 24 h at 37°C. Note that BUB1 was not depleted in these experiments. The number of TUNEL$^+$ cells among more than 200 cells was counted. Bars represent the mean percentages (± SD) of TUNEL$^+$ mitotic cells. Three independent experiments were performed. (F) The BUB1 level of expression in the cells from tumors with CIN was lower than that in the cells from tumors with MIN or that in HeLa cells. Approximately 30 μg of each cell lysate was loaded, and immunoblotting was performed using anti-BUB1 antibody. Anti-GAPDH served as a loading control. (G) Overexpression of BUB1 suppressed CIMD in three colon cancer cell lines with CIN. We transfected each cell line that exhibited CIN with pBI-GFP-BUB1-WT mammalian expression vector that expresses BUB1. At 24 h after AMAXA nucleofector transfection, we incubated cells with Taxol and continued incubation for 24 h. Cells were fixedand only GFP$^+$ cells were detected. We observed that only Taxol-treated and BUB1-expressing cells suppressed CIMD in the condition that induced CIMD in the cells transfected with the GFP control vector. (H) Overexpression of a dominant-negative mutant of Bub1 (Bub1*V400) induces CIMD. We transfected HeLa cells with pBI-GFP-Bub1-V400 mammalian expression vector that expresses the mutant (the N-terminal region of BUB1) that was found in a tumor with CIN (Cahill et al., 1998). At 48 h after transfection, we treated cells with NOC and incubated them for another 24 h. Cells were fixed and only GFP$^+$ cells were detected.

death occurs downstream of BUB1 depletion. However, if that was the case, BUB1 depletion should cause substantial CIMD, which it does not. Also, BUB1 is not required for the kinetochore localization of hNuf2 (Meraldi and Sorger, 2005). Therefore, hNuf2 depletion–induced cell death is unlikely to be CIMD, although further investigation is required. Neither the above-mentioned studies nor the previously described mitotic cell death findings exemplify the CIMD detected by the TUNEL assay during early mitosis and is independent of caspases and p53.

Is CIMD a type of apoptosis?

Some think that apoptosis is a type of cell death that involves caspases (Chipuk and Green, 2005), then CIMD is not a type of apoptosis. However, some think that apoptosis is defined as a physiologic "cell suicide" program characterized by lethal DNA fragmentation (Okada and Mak, 2004). Because mitotic chromosomes are fragmented during CIMD, the cells can no longer survive. Although TUNEL$^+$ chromosomes are observed, there is no apparent reason for the cells to die immediately, unless the DNA becomes fragmented (e.g., only 5% of TUNEL$^+$ metaphase cells had misaligned chromosomes [unpublished data]). Also, this DNA fragmentation occurs rapidly (within 20 min) after the kinetochore–microtubule attachment is disrupted (when the checkpoint fails, death should occur immediately because the checkpoint stops the cell cycle). Therefore, there must be an "active" cell death system to induce DNA fragmentation in the cells that are depleted of BUB1 and have defects in kinetochore–microtubule attachment during mitosis.

AIF and EndoG play important roles in caspase-independent cell death and are released from the mitochondria during CIMD activation. Depletion of EndoG and AIF suppressed DNA fragmentation and rescued the lethality caused by CIMD. Suppression

of DNA fragmentation by depletion of AIF was weaker than that by depletion of EndoG, probably because AIF digests DNA into large molecules (50–100 kb) (Susin et al., 1999).

On the basis of these results, we conclude that CIMD is a previously uncharacterized type of active cell death. We did not observe cytochrome *c* release from the mitochondria during CIMD, which is consistent with CIMD being caspase independent (Cregan et al., 2004).

Our TEM analyses revealed that after CIMD, cells contain increased numbers of abnormal mitochondria, which are seen in apoptotic cells, and autophagosomes, especially in 17-AAG–treated and BUB1-depleted cells. Autophagy promotes cell death when cells are triggered to die, but authentic apoptosis cannot occur (Eskelinen, 2005). Therefore, our TEM analyses support that CIMD is an active cell death. Substantial numbers of holes or vesicles were observed in cells after CIMD occurred, but we do not know how they were generated. Autophagy may generate the holes or vesicles via the autophagy/autolysosome pathway.

Mitotic death pathways

On the basis of our findings and those of others, we propose a model of BUB1 and MAD2 function in the spindle checkpoint pathway to determine the fate of cells with mitotic errors (Fig. 8 A). BUB1 binds kinetochores in mammalian cells before BUBR1 or MAD2 does, and BUB1 is required for the subsequent localization of CENP-F, BUBR1, CENP-E, and MAD2 (Johnson et al., 2004). These findings and ours suggest that BUB1 functions upstream of MAD2 in the checkpoint pathway. When kinetochore–microtubule attachment is defective and BUB1 function is partly altered, cells still undergo arrest in mitosis, but CIMD occurs. Thus, the full activity of BUB1 is required to protect cells from CIMD.

Many tumor cells have a diminished, but not absent, spindle checkpoint response (Kops et al., 2005). In fact, we found that in tumors with CIN BUB1 expression levels were altered, which induced CIMD, and expression of a *Bub1* mutant derived from a tumor with CIN also induced CIMD. One could argue against CIMD being a cellular mechanism that guards against aneuploidy, because CIMD-inducing conditions appear to be rare. However, CIMD occurs in a low percentage of untreated BUB1-depleted cells. Also, CIMD is induced by cold shock (23°C), which is a very common stress in nature. Therefore, we speculate that CIMD is an alternative death pathway that protects cells from aneuploidy and probably from tumorigenesis. This hypothesis should be examined using the mouse model system in vivo.

To evaluate the model that BUB1 determines the fate of cells with defects in kinetochore–microtubule attachment upstream of MAD2, we performed double depletion of BUB1 and MAD2. Approximately 80% of mitotic cells that are BUB1 and MAD2 depleted showed CIMD (Fig. 8 B), and depletion of BUB1 inhibited premature mitotic exit induced by depletion of MAD2 partly (Fig. S4 G), which supports the hypothesis that BUB1 functions earlier than does MAD2.

The mitotic function of p73

The p53-related p73 proteins regulate the development of the central nervous system and the immune system. They also mediate

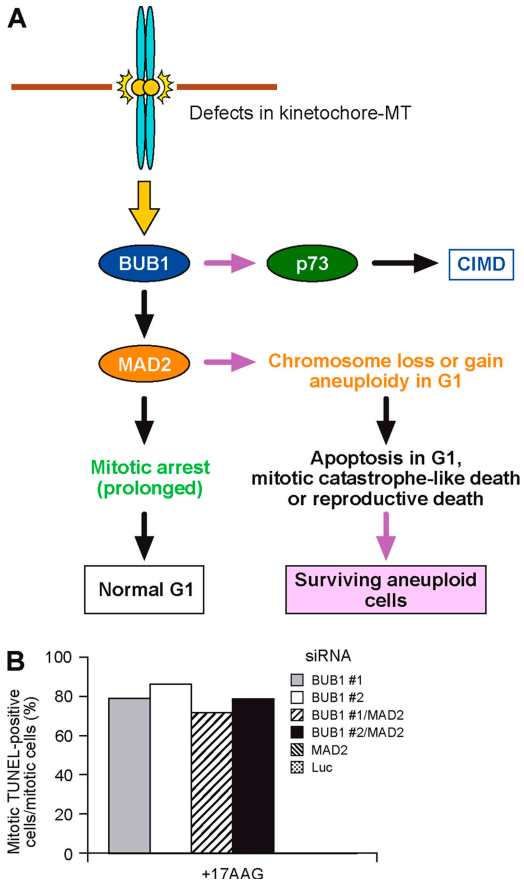

Figure 8. **A model of the checkpoint function of BUB1.** (A) BUB1 functions upstream of MAD2; the checkpoint signaling pathway is presumably more complicated, but the fate (i.e., type of death) of the cells is the focus in this model. Purple arrows indicate the events that occur when the proteins fail to perform their functions. When defects in the kinetochore-microtubule attachment occur in BUB1-depleted cells, the cells enter CIMD. If MAD2 is absent, chromosomes are lost or gained. The resulting aneuploid cells then enter the subsequent G1 phase, and apoptosis, mitotic catastrophe–like death, or reproductive death occurs. (B) If the model in A is correct, then when BUB1 and MAD2 functions are disrupted, CIMD occurs, because BUB1 function is upstream in the pathway. MAD2 depletion did not substantially affect CIMD induced by BUB1 depletion, which strongly supports the model in A.

the cell cycle and apoptosis in response to DNA damage (Ramadan et al., 2005; Coates, 2006). At the G2/M transition, p73 is phosphorylated at Thr-86 by the p34cdc2/cyclin B complex (Fulco et al., 2003). This M phase–specific phosphorylation of p73 generally hinders its transcriptional activity. However, p73-specific transcriptional targets during mitosis such as the cyclin-dependent kinase inhibitor Kip2/p57 exist (Merlo et al., 2005). Therefore, CIMD may be induced by p73-specific transcriptional target proteins during mitosis. DNA microarray analyses should be performed to identify these genes.

MAD2 depletion

The synthetic lethality caused by MAD2 siRNA and 17-AAG or paclitaxel was higher than that induced by BUB1 siRNA, which suggests that, rather than apoptosis or CIMD, another mechanism of death (e.g., reproductive death) occurs in cells treated with 17-AAG or paclitaxel and MAD2 siRNA. Although defects occur

in the kinetochore of 17-AAG–treated cells, MAD2-depleted cells do not arrest in mitosis because of defects in spindle checkpoint activity. Therefore, abnormal chromosome segregation is expected to occur and result in aneuploidy because of the premature exit from mitosis. In fact, the number of abnormal nuclei, including micronuclei, was increased substantially in 17-AAG–treated and MAD2-depleted cells but not in 17-AAG–treated and BUB1-depleted cells. Although these phenotypes are more drastic, they resemble those of MAD2- or BUBR1-depleted cells (Kops et al., 2004). Therefore, mitotic catastrophe–like death that is presumably caused by premature exit from mitosis appears to occur in most MAD2-depleted and 17-AAG– or paclitaxel-treated cells.

Sudo et al. (2004) suggested that inactivation of MAD2 increases cell survival upon paclitaxel treatment (Sudo et al., 2004). This finding is inconsistent with ours. We believe that this difference can be explained by Sudo et al.'s use of 3-(4,5-dimethylthiazol-2-yl)-2,5-diphenyltetrazolium bromide and trypan blue assays to evaluate cell viability, as neither of those methods detect reproductive cell death.

Survivin

The inhibitor of apoptosis protein survivin is also known as a chromosome passenger protein that associates with kinetochores transiently and is required for the spindle checkpoint function (Li et al., 1998; Skoufias et al., 2000; Carvalho et al., 2003; Lens et al., 2003). Disruption of survivin–microtubule interactions inhibits the anti-apoptosis function of survivin and induces caspase-3 activity (Li et al., 1998). Survivin regulates mitochondrial apoptosis and caspase-9 recruitment to the Apaf-1 apoptosome (Marusawa et al., 2003). Therefore, survivin does not appear to be involved in CIMD. Overexpression of survivin does not suppress CIMD (Fig. S5, A and B, available at http://www.jcb.org/cgi/content/full/jcb.200702134/DC1), though it does suppress paclitaxel- or geldanamycin-induced, caspase-mediated apoptosis (Li et al., 1998; Fortugno et al., 2003).

EndoG-null mice

Although EndoG was initially shown to be required for early embryogenesis and normal apoptosis in mice (Zhang et al., 2003), recently reports in *EndoG*-null mice have shown that EndoG is dispensable in embryogenesis and apoptosis (Irvine et al., 2005; David et al., 2006). However, the results from these reports do not exclude the involvement of EndoG in CIMD nor deny the potential significance of CIMD in antitumorigenesis. We showed that EndoG is required for CIMD but redundantly with AIF. *Bub1* transgenic mice did not show increased predisposition to spontaneous tumors (Cowley et al., 2005), raising the possibility that CIMD protects these animals from tumorigenesis. Further investigation is needed to address the function of CIMD in mice with multiple mutations of key factors.

CIMD of tumor cells with CIN treated with microtubule inhibitors or 17-AAG

Successful Phase I trials of 17-AAG have recently been completed; 17-AAG was well tolerated at doses that modulate the level of Hsp90 client proteins (Banerji et al., 2005; Glaze et al., 2005; Goetz et al., 2005; Grem et al., 2005; Ramanathan et al., 2005). CIMD may be a main mechanism by which 17-AAG and microtubule inhibitors kill tumor cells with CIN. The similarity between the cell death response induced by 17-AAG and that induced by microtubule inhibitors, which are classic anti-cancer agents (Mollinedo and Gajate, 2003), suggests that similar mechanisms are involved, although 17-AAG uses multiple mechanisms (Miyata, 2005).

Last but not least, the mitotic index has been used to evaluate spindle checkpoint activity. Our findings suggest that previous studies probably failed to detect defects in the BUB1 pathway, because the mitotic index appears to be normal during CIMD. Thus, the results of those earlier studies, especially those involving tumor cells, should be reevaluated with consideration of the occurrence of CIMD. Furthermore, the detection of CIMD could be a novel method for diagnosing tumors with CIN.

Materials and methods

siRNA

The siRNAs targeting MAD2 and luciferase have been described previously (Elbashir et al., 2001; Martin-Lluesma et al., 2002). We used three BUB1 siRNAs: 5′-GCCUGCCAACCCCUGGGAATT-3′(BUB1siRNA#1), 5′-CAACACUAUACUAACAAGATT-3′(BUB1siRNA#2), and 5′-CCAGGCUGAACCCAGAGAGTT-3′ for the studies described in the main text. Similar data were obtained when these independent sets of siRNAs were used. The siRNA targeting AIF has been described previously (Bidere et al., 2003). We also designed another AIF siRNA: 5′-CUUGUUCCAGCGAUGGCAUUU-3′. Similar data were obtained when these two independent sets of siRNAs were used. We designed three sets of EndoG siRNAs: 5′-AAGAGCCGCGAGUCGUACGUG-3′, 5′-AACGCACCUGUGGAUGAGGCC-3′, and 5′-CGGGCUUCGGGGCUGCUCUUU-3′, and similar data were obtained when these three independent sets of siRNAs were used. The siRNAs targeting MAD2, BUB1, AIF, and EndoG were synthesized by the Hartwell Center for Bioinformatics and Biotechnology at St. Jude Children's Research Hospital (Memphis, TN).

Antibodies

Table S2 lists the antibodies used in this study (available at http://www.jcb.org/cgi/content/full/jcb.200702134/DC1).

Colony outgrowth assay

The colony outgrowth assay was performed as described previously (Blasco et al., 1997; Reilly et al., 2002; Kranc et al., 2003) with a minor modification. HeLa cells were transfected with siRNAs by using Lipofectamine 2000. 24 h after transfection, the cells were incubated with 100 nM 17-AAG or 1.5 nM Taxol for 2 d, and the drug was removed by washing. Transfected cells (including mitotic cells that were recovered from the supernatant; $n = 2{,}000$) were spread in one well of a six-well cluster (Corning Costar) and incubated 12–14 d to allow colony formation. Colonies stained with Giemsa solution (HEMA-QUIK stain solution; Fisher Scientific) were counted. The viability (%) was normalized; the percentage of surviving colonies of untreated cells transfected with control luciferase siRNA was arbitrarily set to 100.

TUNEL assay

48 h after siRNA transfection, HeLa cells, tumor cells with CIN, or tumor cells with MIN were incubated with 500 nM 17-AAG (A.G. Scientific) for 24 h. Cells were fixed with 4% paraformaldehyde in phosphate-buffered saline (pH 7.4), and the TUNEL assay was performed by using an in situ cell death detection system that contained TMR red (Roche).

Caspase assay

HeLa cells were transfected with siRNA, and 48 h later the cells were incubated in 500 nM 17-AAG for 24 h. The FLICA caspase assay was performed by using the carboxyfluorescein FLICA (Poly-Caspases FLICA [FAM-VAD-FMK]) apoptosis detection system (Immunochemistry Technologies, LLC).

Cell culture and transfection

All human cell lines were purchased from American Type Culture Collection (Manassas, VA). HeLa and SW480 cells were cultured in high glucose DME (BioWhittaker) with 10% fetal bovine serum (FBS; Invitrogen); Caco-2

and RKO cells, in Eagle's minimum essential medium (ATCC) with 10% FBS; HT29 and HCT116 cells, in McCoy's 5A medium (ATCC) with 10% FBS; and DLD-1 cells, in RPMI-1640 medium (ATCC) with 10% FBS. All cell lines were grown at 37°C in 5% CO_2 in a humidified incubator. Cells were transfected with annealed double-stranded siRNA or mammalian expression plasmids by using Lipofectamine 2000 (Invitrogen) or Fugene 6 (Roche).

Immunoblotting

The method of immunoblotting has been described in detail elsewhere (Lamb et al., 1995; Kitagawa et al., 1999). Cells were added to lysis buffer A (Panaretou et al., 2002), and the mixture was frozen in liquid nitrogen, thawed, and sonicated. Before electrophoresis, cell lysates were mixed with an equal volume of 2× SDS sample buffer.

Immunofluorescence

Methods of indirect immunofluorescent staining have been described previously (Tugendreich et al., 1995; Yoda et al., 1996), but were slightly modified. HeLa cells were grown for 48 h on coverslip slides (seeding, ~2.0×10^5 cells). Asynchronous populations of HeLa cells were fixed in 4% paraformaldehyde in phosphate-buffered saline at 4°C for 30 min and then treated with 0.5% Triton X-100 in KB (10 mM Tris HCl, pH 7.5, 150 mM NaCl, and 0.5% bovine serum albumin) at room temperature for 30 min. The cells were then incubated with a specific primary antibody for 1 h at 37°C. After the cells were washed once with KB, they were incubated with the fluorescent secondary antibodies fluorescein isothiocyanate–conjugated AffiniPure IgG or Texas red–conjugated AffiniPure IgG (Jackson ImmunoResearch Laboratories) for 1 h at 37°C. Slides were washed once with KB and then incubated in KB containing 0.1 μg/ml DAPI (Sigma-Aldrich). Cells were observed through an Axioskop2 (Carl Zeiss MicroImaging, Inc.) motorized fluorescence microscope equipped with a Plan Apochromat 63× oil immersion lens (Carl Zeiss MicroImaging, Inc.), an HBO 100 microscope illuminator (Attoarc), and a microMAX CCD camera (Princeton Instruments, Inc.). Appropriate filters were used to photograph stained cells. Image acquisition and processing was performed with IP Lab Scientific Imaging Software (Scanalytics). Alternatively, we observed cells through a DM IRE2 motorized fluorescence microscope (Leica) equipped with an HCX PL APO 63× oil immersion lens (Leica), an ARC LAMP power supply HBO100 DC IGN (Ludl Electronic Products, Ltd.), and an ORCA-ER high-resolution digital CCD camera (Hamamatsu). Image acquisition and processing were performed using Openlab version 4 Scientific Imaging Software (Improvision).

DNA fragmentation assay

A DNA fragmentation assay was performed as described previously (Sonoda et al., 1997, 1999, 2000). In brief, cells were gently lysed for 30 min at room temperature in buffer containing 5 mM Tris-HCl (pH 7.4), 20 mM EDTA, and 0.5% Triton X-100. After centrifugation at 15,000 rpm for 15 min, supernatants containing soluble, fragmented DNA were collected and treated with RNase (20 μg/ml; Sigma-Aldrich) and then with protease K (20 μg/ml). DNA fragments were precipitated in 99% ethanol. Samples were then subjected to electrophoresis in a 2% agarose gel and visualized by staining with ethidium bromide.

Time-lapse imaging and analysis

HeLa cells were plated on 10-mm-diameter tissue culture plates with glass bottoms (MatTek Corp.) that had been coated with poly-D-lysine. Cells were then transfected with either human BUB1 siRNA or luciferase siRNA using Lipofectamine 2000 (Invitrogen). After 48–54 h, cells were incubated with 1 mM ICRF-187 (cardioxane; Chiron Corp.). After 54 h, cells were transferred to L15 Leibovitz medium to which 2.05 mM L-glutamine (HyClone) had been added. The medium was then supplemented with 10% fetal bovine serum and 1% penicillin-streptomycin (both from Invitrogen). At the same time cells were coincubated with 1 mM ICRF-187 and 500 nM 17-AAG, over which Sigma mineral oil had been placed. Cells were then maintained at 37°C. Phase-contrast images were captured every half hour for 24 h (after 54–78 h of transfection). Cells were imaged on a DM IRE2 motorized microscope equipped with an HCX PL FLUOT AR 40× lens (Leica), an ARC LAMP power supply HBO100 DC IGN (Ludl Electronic Products, Ltd.), and an ORCA-ER high-resolution digital CCD (charge-coupled device) camera (Hamamatsu). Images were acquired and processed using Openlab version 4.0.4 Scientific Imaging Software (Improvision). Pictures images were saved in Openlab's LIFF format, converted to TIFF format, and then exported to Adobe Photoshop.

Electron microscopy

Mitotic HeLa cells were collected by gentle pipetting and fixed briefly with a 37°C solution of 2% paraformaldehyde, 2.5% glutaraldehyde in 0.15 M sodium cacodylate (pH 7.4). Low-melting point agarose (4%) was mixed with an equal volume of fixed cells and was transferred to a box with cold packs for shipment to National Center for Microscopy and Imaging Research (NCMIR). The samples arrived cold at NCMIR and were rinsed three times for 5 min with 0.15 M sodium cacodylate plus 3 mM calcium chloride (pH 7.4) on ice and then post-fixed with 1% osmium tetroxide, 0.8% potassium ferrocyanide (Sigma-Aldrich), and 3 mM calcium chloride in 0.15 M sodium cacodylate (pH 7.4) for 2 h and then washed three times for 5 min with ice-cold distilled water. The cells were stained for 2 h with 2% uranyl acetate at 4°C, dehydrated in graded ethanol incubations, and embedded in Durcupan resin (Fluka). Ultrathin (80 nm) sections were post-stained with uranyl acetate for 10 min and Sato lead for 2 min and imaged with a JEOL 1200FX transmission electron microscope operated at 80 kV. Mitotic cells were imaged on film at 3,000–5,000 magnification on a JEOL 1200FX electron microscope. The negatives were digitized at 1,800 dpi using a Nikon Coolscan system, giving an image size of 4034 × 6009 pixel array. All reagents were purchased from TED PELLA, Inc., unless otherwise indicated.

Online supplemental material

Fig. S1A shows that overexpression of BUB1 can suppress CIMD when siRNA that targets the 3′-UTR region of BUB1 and 17-AAG were used. Fig. S1 B shows a control immunoblot to confirm the transfection of the plasmids that were used in Fig. S1A and Fig. 7 H. Fig. S1 C shows that increased concentrations of paclitaxel (Taxol; 10–1,000 nM) treatment of BUB1-depleted cells do not affect the levels of mitotic TUNEL-positive (black bars) cells substantially. Fig. S1 D shows determination of the concentration of inhibitors needed to suppress caspase activity in HeLa cells. Fig. S1 E shows that CIMD is independent of p53. Fig. S1 F shows overexpression of p73DD. Fig. S2 A shows CIMD did not occur in $p73^{-/-}$ MEF cells efficiently. Fig. S2 B shows AIF and EndoG (green) are colocalized with mitochondria (red). Fig. S2 C shows protein depletion by AIF siRNA and EndoG siRNA. Fig. S2 D shows mitotic arrest caused by 17-AAG was not affected by either AIF siRNA #1 or #2 or EndoG siRNA #1 or #2. Fig. S2 E shows TUNEL assay of mitotic BUB1-depleted and ICRF187-treated cells indicated that ICRF187 did not induce CIMD in BUB1-depleted cells. Fig. S2 F shows kinetics of Endo G release and TUNEL signals after addition of 17-AAG or microtubule inhibitors to BUB1-depleted cells. Fig. S3 (A–C) shows electron microscopy images of BUB1-depleted cells that were treated with 17-AAG. Fig. S4 A shows depletion of BUB1 by using various sets of siRNAs. Fig. S4 B shows the mitotic index is the same as that shown in Fig. 2 C. Mitotic TUNEL-positive cells were not observed when MAD2 was partially depleted. Fig. S4 C shows immunoblotting of HeLa cells that were transfected with the indicated plasmid vectors by using anti-BUB1 antibody. Fig. S4 D shows CIMD induced by 17-AAG treatment did not activate caspases in tumor cells with CIN. Fig. S4 E shows CIMD induced by treatment with 17-AAG was not suppressed by Pan-caspase inhibitors VAD (zVAD; 50 μM) or BAF (50 μM). Fig. S4 (F and G) shows overexpression of survivin did not inhibit CIMD. Online supplemental material is available at http://www.jcb.org/cgi/content/full/jcb.200702134/DC1.

We thank D.R. Green, C.L. Rieder, M. Kastan, V. Measday, J. Lahti, T.J. Yen, J. Partridge, P. Bansal, S. Ohta, and R. Kitagawa for their helpful comments; S. Moshiach, M. Sugimoto, and K. Tago for stimulating conversation and advice; A. Rashid and E. Law for their technical assistance; B. Vogelstein, M. Kastan, J. Lahti, T.J. Yen, and S.S. Taylor for their generous gifts of reagents; and J.C. Jones and A.J. McArthur for editing this manuscript.

This work was supported by the Cancer Center Support grant CA21765 from the National Cancer Institute, by NIH grant GM68418, by Susan G. Komen grant BCTR30506, and by the American Lebanese Syrian Associated Charities (ALSAC). Part of the work was performed at the NCMIR supported by NIH grant RR04050 to M.H. Ellisman.

Submitted: 20 February 2007
Accepted: 18 June 2007

References

Asnaghi, L., A. Calastretti, A. Bevilacqua, I. D'Agnano, G. Gatti, G. Canti, D. Delia, S. Capaccioli, and A. Nicolin. 2004. Bcl-2 phosphorylation and apoptosis activated by damaged microtubules require mTOR and are regulated by Akt. *Oncogene.* 23:5781–5791.

Babu, J.R., K.B. Jeganathan, D.J. Baker, X. Wu, N. Kang-Decker, and J.M. van Deursen. 2003. Rae1 is an essential mitotic checkpoint regulator that

cooperates with Bub3 to prevent chromosome missegregation. *J. Cell Biol.* 160:341–353.

Banerji, U., A. O'Donnell, M. Scurr, S. Pacey, S. Stapleton, Y. Asad, L. Simmons, A. Maloney, F. Raynaud, M. Campbell, et al. 2005. Phase I pharmacokinetic and pharmacodynamic study of 17-allylamino, 17-demethoxygeldanamycin in patients with advanced malignancies. *J. Clin. Oncol.* 23:4152–4161.

Barni, S., L. Sciola, A. Spano, and P. Pippia. 1996. Static cytofluorometry and fluorescence morphology of mitochondria and DNA in proliferating fibroblasts. *Biotech. Histochem.* 71:66–70.

Barsoum, M.J., H. Yuan, A.A. Gerencser, G. Liot, Y. Kushnareva, S. Graber, I. Kovacs, W.D. Lee, J. Waggoner, J. Cui, et al. 2006. Nitric oxide-induced mitochondrial fission is regulated by dynamin-related GTPases in neurons. *EMBO J.* 25:3900–3911.

Basu, J., H. Bousbaa, E. Logarinho, Z. Li, B.C. Williams, C. Lopes, C.E. Sunkel, and M.L. Goldberg. 1999. Mutations in the essential spindle checkpoint gene bub1 cause chromosome missegregation and fail to block apoptosis in *Drosophila*. *J. Cell Biol.* 146:13–28.

Bidere, N., H.K. Lorenzo, S. Carmona, M. Laforge, F. Harper, C. Dumont, and A. Senik. 2003. Cathepsin D triggers Bax activation, resulting in selective apoptosis-inducing factor (AIF) relocation in T lymphocytes entering the early commitment phase to apoptosis. *J. Biol. Chem.* 278:31401–31411.

Blank, M., Y. Lerenthal, L. Mittelman, and Y. Shiloh. 2006. Condensin I recruitment and uneven chromatin condensation precede mitotic cell death in response to DNA damage. *J. Cell Biol.* 174:195–206.

Blasco, M.A., H.W. Lee, M.P. Hande, E. Samper, P.M. Lansdorp, R.A. DePinho, and C.W. Greider. 1997. Telomere shortening and tumor formation by mouse cells lacking telomerase RNA. *Cell.* 91:25–34.

Burns, T.F., P. Fei, K.A. Scata, D.T. Dicker, and W.S. El-Deiry. 2003. Silencing of the novel p53 target gene Snk/Plk2 leads to mitotic catastrophe in paclitaxel (taxol)-exposed cells. *Mol. Cell. Biol.* 23:5556–5571.

Cahill, D.P., C. Lengauer, J. Yu, G.J. Riggins, J.K. Willson, S.D. Markowitz, K.W. Kinzler, and B. Vogelstein. 1998. Mutations of mitotic checkpoint genes in human cancers. *Nature.* 392:300–303.

Carvalho, A., M. Carmena, C. Sambade, W.C. Earnshaw, and S.P. Wheatley. 2003. Survivin is required for stable checkpoint activation in taxol-treated HeLa cells. *J. Cell Sci.* 116:2987–2998.

Castedo, M., J.L. Perfettini, T. Roumier, K. Andreau, R. Medema, and G. Kroemer. 2004. Cell death by mitotic catastrophe: a molecular definition. *Oncogene.* 23:2825–2837.

Chipuk, J.E., and D.R. Green. 2005. Do inducers of apoptosis trigger caspase-independent cell death? *Nat. Rev. Mol. Cell Biol.* 6:268–275.

Coates, P. 2006. Regulating p73 isoforms in human tumours. *J. Pathol.* 210:385–389.

Cowley, D.O., G.W. Muse, and T. Van Dyke. 2005. A dominant interfering Bub1 mutant is insufficient to induce or alter thymic tumorigenesis in vivo, even in a sensitized genetic background. *Mol. Cell. Biol.* 25:7796–7802.

Cregan, S.P., A. Fortin, J.G. MacLaurin, S.M. Callaghan, F. Cecconi, S.W. Yu, T.M. Dawson, V.L. Dawson, D.S. Park, G. Kroemer, and R.S. Slack. 2002. Apoptosis-inducing factor is involved in the regulation of caspase-independent neuronal cell death. *J. Cell Biol.* 158:507–517.

Cregan, S.P., V.L. Dawson, and R.S. Slack. 2004. Role of AIF in caspase-dependent and caspase-independent cell death. *Oncogene.* 23:2785–2796.

Dai, W., Q. Wang, T. Liu, M. Swamy, Y. Fang, S. Xie, R. Mahmood, Y.M. Yang, M. Xu, and C.V. Rao. 2004. Slippage of mitotic arrest and enhanced tumor development in mice with BubR1 haploinsufficiency. *Cancer Res.* 64:440–445.

David, K.K., M. Sasaki, S.W. Yu, T.M. Dawson, and V.L. Dawson. 2006. EndoG is dispensable in embryogenesis and apoptosis. *Cell Death Differ.* 13:1147–1155.

DeLuca, J.G., B. Moree, J.M. Hickey, J.V. Kilmartin, and E.D. Salmon. 2002. hNuf2 inhibition blocks stable kinetochore-microtubule attachment and induces mitotic cell death in HeLa cells. *J. Cell Biol.* 159:549–555.

Dobles, M., V. Liberal, M.L. Scott, R. Benezra, and P.K. Sorger. 2000. Chromosome missegregation and apoptosis in mice lacking the mitotic checkpoint protein Mad2. *Cell.* 101:635–645.

Elbashir, S.M., J. Harborth, W. Lendeckel, A. Yalcin, K. Weber, and T. Tuschl. 2001. Duplexes of 21-nucleotide RNAs mediate RNA interference in cultured mammalian cells. *Nature.* 411:494–498.

Eskelinen, E.L. 2005. Doctor Jekyll and Mister Hyde: autophagy can promote both cell survival and cell death. *Cell Death Differ.* 12(Suppl 2): 1468–1472.

Fortugno, P., E. Beltrami, J. Plescia, J. Fontana, D. Pradhan, P.C. Marchisio, W.C. Sessa, and D.C. Altieri. 2003. Regulation of survivin function by Hsp90. *Proc. Natl. Acad. Sci. USA.* 100:13791–13796.

Fulco, M., A. Costanzo, P. Merlo, R. Mangiacasale, S. Strano, G. Blandino, C. Balsano, P. Lavia, and M. Levrero. 2003. p73 is regulated by phosphorylation at the G2/M transition. *J. Biol. Chem.* 278:49196–49202.

Glaze, E.R., A.L. Lambert, A.C. Smith, J.G. Page, W.D. Johnson, D.L. McCormick, A.P. Brown, B.S. Levine, J.M. Covey, M.J. Egorin, et al. 2005. Preclinical toxicity of a geldanamycin analog, 17-(dimethylaminoethylamino)-17-demethoxygeldanamycin (17-DMAG), in rats and dogs: potential clinical relevance. *Cancer Chemother Pharmacol.* 56:637–647.

Goetz, M.P., D. Toft, J. Reid, M. Ames, B. Stensgard, S. Safgren, A.A. Adjei, J. Sloan, P. Atherton, V. Vasile, et al. 2005. Phase I trial of 17-allylamino-17-demethoxygeldanamycin in patients with advanced cancer. *J. Clin. Oncol.* 23:1078–1087.

Grem, J.L., G. Morrison, X.D. Guo, E. Agnew, C.H. Takimoto, R. Thomas, E. Szabo, L. Grochow, F. Grollman, J.M. Hamilton, et al. 2005. Phase I and pharmacologic study of 17-(allylamino)-17-demethoxygeldanamycin in adult patients with solid tumors. *J. Clin. Oncol.* 23:1885–1893.

Hoppe-Seyler, F., and K. Butz. 1993. Repression of endogenous p53 transactivation function in HeLa cervical carcinoma cells by human papillomavirus type 16 E6, human mdm-2, and mutant p53. *J. Virol.* 67:3111–3117.

Hoyt, M.A., L. Totis, and B.T. Roberts. 1991. *S. cerevisiae* genes required for cell cycle arrest in response to loss of microtubule function. *Cell.* 66:507–517.

Hyland, K.M., J. Kingsbury, D. Koshland, and P. Hieter. 1999. Ctf19p: A novel kinetochore protein in *Saccharomyces cerevisiae* and a potential link between the kinetochore and mitotic spindle. *J. Cell Biol.* 145:15–28.

Irvine, R.A., N. Adachi, D.K. Shibata, G.D. Cassell, K. Yu, Z.E. Karanjawala, C.L. Hsieh, and M.R. Lieber. 2005. Generation and characterization of endonuclease G null mice. *Mol. Cell. Biol.* 25:294–302.

Irwin, M., M.C. Marin, A.C. Phillips, R.S. Seelan, D.I. Smith, W. Liu, E.R. Flores, K.Y. Tsai, T. Jacks, K.H. Vousden, and W.G. Kaelin Jr. 2000. Role for the p53 homologue p73 in E2F-1-induced apoptosis. *Nature.* 407:645–648.

Johnson, V.L., M.I. Scott, S.V. Holt, D. Hussein, and S.S. Taylor. 2004. Bub1 is required for kinetochore localization of BubR1, Cenp-E, Cenp-F and Mad2, and chromosome congression. *J. Cell Sci.* 117:1577–1589.

Joza, N., S.A. Susin, E. Daugas, W.L. Stanford, S.K. Cho, C.Y. Li, T. Sasaki, A.J. Elia, H.Y. Cheng, L. Ravagnan, et al. 2001. Essential role of the mitochondrial apoptosis-inducing factor in programmed cell death. *Nature.* 410:549–554.

Kitagawa, K., and P. Hieter. 2001. Evolutionary conservation between budding yeast and human kinetochores. *Nat. Rev. Mol. Cell Biol.* 2:678–687.

Kitagawa, K., D. Skowyra, S.J. Elledge, J.W. Harper, and P. Hieter. 1999. SGT1 encodes an essential component of the yeast kinetochore assembly pathway and a novel subunit of the SCF ubiquitin ligase complex. *Mol. Cell.* 4:21–33.

Kops, G.J., D.R. Foltz, and D.W. Cleveland. 2004. Lethality to human cancer cells through massive chromosome loss by inhibition of the mitotic checkpoint. *Proc. Natl. Acad. Sci. USA.* 101:8699–8704.

Kops, G.J., B.A. Weaver, and D.W. Cleveland. 2005. On the road to cancer: aneuploidy and the mitotic checkpoint. *Nat. Rev. Cancer.* 5:773–785.

Kranc, K.R., S.D. Bamforth, J. Braganca, C. Norbury, M. van Lohuizen, and S. Bhattacharya. 2003. Transcriptional coactivator Cited2 induces Bmi1 and Mel18 and controls fibroblast proliferation via Ink4a/ARF. *Mol. Cell. Biol.* 23:7658–7666.

Lamb, J.R., S. Tugendreich, and P. Hieter. 1995. Tetratrico peptide repeat interactions: to TPR or not to TPR? *Trends Biochem. Sci.* 20:257–259.

Lens, S.M., R.M. Wolthuis, R. Klompmaker, J. Kauw, R. Agami, T. Brummelkamp, G. Kops, and R.H. Medema. 2003. Survivin is required for a sustained spindle checkpoint arrest in response to lack of tension. *EMBO J.* 22:2934–2947.

Li, F., G. Ambrosini, E.Y. Chu, J. Plescia, S. Tognin, P.C. Marchisio, and D.C. Altieri. 1998. Control of apoptosis and mitotic spindle checkpoint by survivin. *Nature.* 396:580–584.

Li, R., and A.W. Murray. 1991. Feedback control of mitosis in budding yeast. *Cell.* 66:519–531.

Li, W., and D.W. Hoffman. 2001. Structure and dynamics of translation initiation factor aIF-1A from the archaeon Methanococcus jannaschii determined by NMR spectroscopy. *Protein Sci.* 10:2426–2438.

Martin-Lluesma, S., V.M. Stucke, and E.A. Nigg. 2002. Role of Hec1 in spindle checkpoint signaling and kinetochore recruitment of Mad1/Mad2. *Science.* 297:2267–2270.

Marusawa, H., S. Matsuzawa, K. Welsh, H. Zou, R. Armstrong, I. Tamm, and J.C. Reed. 2003. HBXIP functions as a cofactor of survivin in apoptosis suppression. *EMBO J.* 22:2729–2740.

Meraldi, P., and P.K. Sorger. 2005. A dual role for Bub1 in the spindle checkpoint and chromosome congression. *EMBO J.* 24:1621–1633.

Merlo, P., M. Fulco, A. Costanzo, R. Mangiacasale, S. Strano, G. Blandino, Y. Taya, P. Lavia, and M. Levrero. 2005. A role of p73 in mitotic exit. *J. Biol. Chem.* 280:30354–30360.

Michel, L.S., V. Liberal, A. Chatterjee, R. Kirchwegger, B. Pasche, W. Gerald, M. Dobles, P.K. Sorger, V.V. Murty, and R. Benezra. 2001. MAD2

haplo-insufficiency causes premature anaphase and chromosome instability in mammalian cells. *Nature.* 409:355–359.

Miyata, Y. 2005. Hsp90 inhibitor geldanamycin and its derivatives as novel cancer chemotherapeutic agents. *Curr. Pharm. Des.* 11:1131–1138.

Mollinedo, F., and C. Gajate. 2003. Microtubules, microtubule-interfering agents and apoptosis. *Apoptosis.* 8:413–450.

Niikura, Y., S. Ohta, K.J. Vandenbeldt, R. Abdulle, B.F. McEwen, and K. Kitagawa. 2006. 17-AAG, an Hsp90 inhibitor, causes kinetochore defects: a novel mechanism by which 17-AAG inhibits cell proliferation. *Oncogene.* 25:4133–4146.

Nitta, M., O. Kobayashi, S. Honda, T. Hirota, S. Kuninaka, T. Marumoto, Y. Ushio, and H. Saya. 2004. Spindle checkpoint function is required for mitotic catastrophe induced by DNA-damaging agents. *Oncogene.* 23:6548–6558

Ohshima, K., S. Haraoka, S. Yoshioka, M. Hamasaki, T. Fujiki, J. Suzumiya, C. Kawasaki, M. Kanda, and M. Kikuchi. 2000. Mutation analysis of mitotic checkpoint genes (hBUB1 and hBUBR1) and microsatellite instability in adult T-cell leukemia/lymphoma. *Cancer Lett.* 158:141–150.

Okada, H., and T.W. Mak. 2004. Pathways of apoptotic and non-apoptotic death in tumour cells. *Nat. Rev. Cancer.* 4:592–603.

Panaretou, B., G. Siligardi, P. Meyer, A. Maloney, J.K. Sullivan, S. Singh, S.H. Millson, P.A. Clarke, S. Naaby-Hansen, R. Stein, et al. 2002. Activation of the ATPase activity of hsp90 by the stress-regulated cochaperone aha1. *Mol. Cell.* 10:1307–1318.

Perez, G.I., B.M. Acton, A. Jurisicova, G.A. Perkins, A. White, J. Brown, A.M. Trbovich, M.-R. Kim, R. Fissore, J. Xu, et al. 2007. Genetic variance modifies apoptosis susceptibility in mature oocytes via alterations in DNA repair capacity and mitochondrial ultrastructure. *Cell Death Differ.* 14:524–533.

Perkins, G.A., M.H. Ellisman, and D.A. Fox. 2004. The structure-function correlates of mammalian rod and cone photoreceptor mitochondria: observations and unanswered questions. *Mitochondrion.* 4:695–703.

Ramadan, S., A. Terrinoni, M.V. Catani, A.E. Sayan, R.A. Knight, M. Mueller, P.H. Krammer, G. Melino, and E. Candi. 2005. p73 induces apoptosis by different mechanisms. *Biochem. Biophys. Res. Commun.* 331:713–717.

Ramanathan, R.K., D.L. Trump, J.L. Eiseman, C.P. Belani, S.S. Agarwala, E.G. Zuhowski, J. Lan, D.M. Potter, S.P. Ivy, S. Ramalingam, et al. 2005. Phase I pharmacokinetic-pharmacodynamic study of 17-(allylamino)-17-demethoxygeldanamycin (17AAG, NSC 330507), a novel inhibitor of heat shock protein 90, in patients with refractory advanced cancers. *Clin. Cancer Res.* 11:3385–3391.

Reilly, P.T., J. Wysocka, and W. Herr. 2002. Inactivation of the retinoblastoma protein family can bypass the HCF-1 defect in tsBN67 cell proliferation and cytokinesis. *Mol. Cell. Biol.* 22:6767–6778.

Rieder, C.L., and R.W. Cole. 2002. Cold-shock and the Mammalian cell cycle. *Cell Cycle.* 1:169–175.

Rieder, C.L., and H. Maiato. 2004. Stuck in division or passing through: what happens when cells cannot satisfy the spindle assembly checkpoint. *Dev. Cell.* 7:637–651.

Ru, H.Y., R.L. Chen, W.C. Lu, and J.H. Chen. 2002. hBUB1 defects in leukemia and lymphoma cells. *Oncogene.* 21:4673–4679.

Saeki, A., S. Tamura, N. Ito, S. Kiso, Y. Matsuda, I. Yabuuchi, S. Kawata, and Y. Matsuzawa. 2002. Frequent impairment of the spindle assembly checkpoint in hepatocellular carcinoma. *Cancer.* 94:2047–2054.

Shigeishi, H., N. Oue, H. Kuniyasu, A. Wakikawa, H. Yokozaki, T. Ishikawa, and W. Yasui. 2001. Expression of Bub1 gene correlates with tumor proliferating activity in human gastric carcinomas. *Pathobiology.* 69:24–29.

Skoufias, D.A., C. Mollinari, F.B. Lacroix, and R.L. Margolis. 2000. Human survivin is a kinetochore-associated passenger protein. *J. Cell Biol.* 151:1575–1582.

Skoufias, D.A., F.B. Lacroix, P.R. Andreassen, L. Wilson, and R.L. Margolis. 2004. Inhibition of DNA decatenation, but not DNA damage, arrests cells at metaphase. *Mol. Cell.* 15:977–990.

Sonoda, Y., T. Kasahara, E. Yokota-Aizu, M. Ueno, and S. Watanabe. 1997. A suppressive role of p125FAK protein tyrosine kinase in hydrogen peroxide-induced apoptosis of T98G cells. *Biochem. Biophys. Res. Commun.* 241:769–774.

Sonoda, Y., S. Watanabe, Y. Matsumoto, E. Aizu-Yokota, and T. Kasahara. 1999. FAK is the upstream signal protein of the phosphatidylinositol 3-kinase-Akt survival pathway in hydrogen peroxide-induced apoptosis of a human glioblastoma cell line. *J. Biol. Chem.* 274:10566–10570.

Sonoda, Y., Y. Matsumoto, M. Funakoshi, D. Yamamoto, S.K. Hanks, and T. Kasahara. 2000. Anti-apoptotic role of focal adhesion kinase (FAK). Induction of inhibitor-of-apoptosis proteins and apoptosis suppression by the overexpression of FAK in a human leukemic cell line, HL-60. *J. Biol. Chem.* 275:16309–16315.

Sudo, T., M. Nitta, H. Saya, and N.T. Ueno. 2004. Dependence of paclitaxel sensitivity on a functional spindle assembly checkpoint. *Cancer Res.* 64:2502–2508.

Susin, S.A., H.K. Lorenzo, N. Zamzami, I. Marzo, B.E. Snow, G.M. Brothers, J. Mangion, E. Jacotot, P. Costantini, M. Loeffler, et al. 1999. Molecular characterization of mitochondrial apoptosis-inducing factor. *Nature.* 397:441–446.

Susin, S.A., E. Daugas, L. Ravagnan, K. Samejima, N. Zamzami, M. Loeffler, P. Costantini, K.F. Ferri, T. Irinopoulou, M.C. Prevost, et al. 2000. Two distinct pathways leading to nuclear apoptosis. *J. Exp. Med.* 192:571–580.

Taylor, S.S., and F. McKeon. 1997. Kinetochore localization of murine Bub1 is required for normal mitotic timing and checkpoint response to spindle damage. *Cell.* 89:727–735.

Tong, A.H., M. Evangelista, A.B. Parsons, H. Xu, G.D. Bader, N. Page, M. Robinson, S. Raghibizadeh, C.W. Hogue, H. Bussey, et al. 2001. Systematic genetic analysis with ordered arrays of yeast deletion mutants. *Science.* 294:2364–2368.

Tsukasaki, K., C.W. Miller, E. Greenspun, S. Eshaghian, H. Kawabata, T. Fujimoto, M. Tomonaga, C. Sawyers, J.W. Said, and H.P. Koeffler. 2001. Mutations in the mitotic check point gene, MAD1L1, in human cancers. *Oncogene.* 20:3301–3305.

Tugendreich, S., J. Tomkiel, W. Earnshaw, and P. Hieter. 1995. CDC27Hs colocalizes with CDC16Hs to the centrosome and mitotic spindle and is essential for the metaphase to anaphase transition. *Cell.* 81:261–268.

van Loo, G., X. Saelens, F. Matthijssens, P. Schotte, R. Beyaert, W. Declercq, and P. Vandenabeele. 2002. Caspases are not localized in mitochondria during life or death. *Cell Death Differ.* 9:1207–1211.

Wang, X., D.Y. Jin, R.W. Ng, H. Feng, Y.C. Wong, A.L. Cheung, and S.W. Tsao. 2002. Significance of MAD2 expression to mitotic checkpoint control in ovarian cancer cells. *Cancer Res.* 62:1662–1668.

Wells, W.A., and A.W. Murray. 1996. Aberrantly segregating centromeres activate the spindle assembly checkpoint in budding yeast. *J. Cell Biol.* 133:75–84.

Woods, C.M., J. Zhu, P.A. McQueney, D. Bollag, and E. Lazarides. 1995. Taxol-induced mitotic block triggers rapid onset of a p53-independent apoptotic pathway. *Mol. Med.* 1:506–526.

Yang, Z., J. Guo, Q. Chen, C. Ding, J. Du, and X. Zhu. 2005. Silencing mitosin induces misaligned chromosomes, premature chromosome decondensation before anaphase onset, and mitotic cell death. *Mol. Cell. Biol.* 25:4062–4074.

Yoda, K., T. Nakamura, H. Masumoto, N. Suzuki, K. Kitagawa, M. Nakano, A. Shinjo, and T. Okazaki. 1996. Centromere protein B of African green monkey cells: gene structure, cellular expression, and centromeric localization. *Mol. Cell. Biol.* 16:5169–5177.

Yoon, D.S., R.P. Wersto, W. Zhou, F.J. Chrest, E.S. Garrett, T.K. Kwon, and E. Gabrielson. 2002. Variable levels of chromosomal instability and mitotic spindle checkpoint defects in breast cancer. *Am. J. Pathol.* 161:391–397.

Yu, S.W., H. Wang, M.F. Poitras, C. Coombs, W.J. Bowers, H.J. Federoff, G.G. Poirier, T.M. Dawson, and V.L. Dawson. 2002. Mediation of poly(ADP-ribose) polymerase-1-dependent cell death by apoptosis-inducing factor. *Science.* 297:259–263.

Zhang, J., M. Dong, L. Li, Y. Fan, P. Pathre, J. Dong, D. Lou, J.M. Wells, D. Olivares-Villagomez, L. Van Kaer, et al. 2003. Endonuclease G is required for early embryogenesis and normal apoptosis in mice. *Proc. Natl. Acad. Sci. USA.* 100:15782–15787.